



HAL
open science

Microstructures and physical properties in carbonate rocks: A comprehensive review

J.B. Regnet, C. David, P. Robion, Beatriz Menendez

► To cite this version:

J.B. Regnet, C. David, P. Robion, Beatriz Menendez. Microstructures and physical properties in carbonate rocks: A comprehensive review. *Marine and Petroleum Geology*, 2019, 103, pp.366-376. 10.1016/j.marpetgeo.2019.02.022 . hal-03266035

HAL Id: hal-03266035

<https://hal.science/hal-03266035v1>

Submitted on 22 Oct 2021

HAL is a multi-disciplinary open access archive for the deposit and dissemination of scientific research documents, whether they are published or not. The documents may come from teaching and research institutions in France or abroad, or from public or private research centers.

L'archive ouverte pluridisciplinaire **HAL**, est destinée au dépôt et à la diffusion de documents scientifiques de niveau recherche, publiés ou non, émanant des établissements d'enseignement et de recherche français ou étrangers, des laboratoires publics ou privés.



Distributed under a Creative Commons Attribution - NonCommercial 4.0 International License

1 **Microstructures and physical properties in carbonate rocks :** 2 **a comprehensive review**

3 ***J.B. Regnet^{a,b}, C. David^a, P. Robion^a, B. Menéndez^a***

4 a - Laboratoire Géosciences et Environnement Cergy, Université de Cergy-Pontoise, France

5 b - Formerly at Department of Civil Engineering and Applied Mechanics, McGill University, Montreal, Canada

6 Corresponding Author : jean-baptiste.regnet@u-cergy.fr. Laboratoire Géosciences et Environnement Cergy, Maison
7 Internationale de la Recherche, Université de Cergy-Pontoise, 1 rue René Descartes, 95000 Neuville sur Oise, France.

8

9 **Abstract**

10 Carbonate rocks are well-known to be tremendously heterogeneous. They mainly consist of component particles
11 (from biological and non-biological origin) embedded in a lime-mud matrix and/or in a cement (composed of
12 even smaller particles). The size, shape, density and spatial arrangement of those particles, alongside with natural
13 fractures and cracks (although those are certainly not exclusive to carbonate rocks), define a microstructural
14 pattern that is known to have a great influence on rock physical properties.

15 Thus, to understand carbonate rock systems at large scales (formation, reservoir...), geophysicists have to study
16 them at the pore scale, hoping to resolve the so-called "upscaling" problem. With this in mind, unravelling and
17 identifying the relations between physical properties and carbonate rock microstructures is paramount for a
18 global comprehension of a carbonate rock system. Since the late nineties, several research groups and authors
19 have worked on documenting and providing significant insights into the microstructural parameters controlling
20 the physical response of several rock properties (porosity, permeability, electrical conductivity, elastic, seismic
21 and mechanical properties...) in carbonates. This article proposes a review of this specialized literature, from the
22 early and recent contributions in rock physics, with emphasis on the recent studies on carbonate rocks from the
23 Paris basin.

24

25 **Keywords:** Carbonate rocks, microstructures, petrophysical properties

26

27 **1. Introduction**

1 Further knowledge of rock physical and mechanical properties is necessary, and has been a long-time
2 major focus of geophysics. The implications are wide, from fundamental science to applied geology,
3 involving exploration and production of fossil energies, groundwater, geological storage of wastes,
4 earthquakes prediction, and on larger scales the behavior of the Earth's lithosphere. The Earth's crust
5 is a very complex geological domain, where the physical properties of rocks are very heterogeneous
6 and sometimes anisotropic. Those heterogeneities are often a reflection of the complex association
7 between microstructures, inherited from sediment deposition and diagenesis conditions, stress state,
8 pressure and temperature conditions, or the nature of saturating fluids. This statement is even more
9 obvious if we consider the carbonate rocks, which are inherently heterogeneous rocks. They mainly
10 consist of component particles (from biological and non-biological origin) embedded in a lime-mud
11 matrix and/or in a cement (composed of even smaller particles). Those elements generally undergo an
12 intense diagenesis over time because of the very high chemical sensitivity of the carbonate mineral
13 species (calcite, aragonite and dolomite). This usually results in a complex medium, with strong
14 impacts on rock physical properties. The microstructures resulting from all these mechanisms often
15 have a coupling effect within the rocks, and lead to modify both their solid framework and porous
16 network irreversibly.

17 Thus, to understand carbonate rock systems at large scales (formation, reservoir...), geophysicists have
18 to study them at the pore scale, hoping to resolve the so-called "upscaling" problem. With this in
19 mind, unravelling and identifying the relations between physical properties and carbonate rock
20 microstructures is paramount for a global comprehension of a carbonate rock system. This statement
21 however, is far more easily said than done because of the wide heterogeneity of microstructures
22 encountered in those media, and attempting to make sense of their physical properties can be a major
23 challenge. Until today, and despite the many publications on this topic, only a few general
24 compilations exist about all the factors that are known to control those physical parameters. This
25 review attempts to fill this gap, by proposing a comprehensive review of this specialized literature,
26 from the early and recent contributions in rock physics, with emphasis on the recent studies on
27 carbonate rocks from the Paris basin, developed by the research group at the Geosciences and
28 Environment laboratory at the University of Cergy-Pontoise. Effects related to temperature, stress,

1 frequency and the nature of the saturating fluid will not be treated here, as they are more linked to the
2 environmental conditions and measurement than to intrinsic rock properties.

3

4 **2. Microstructures classifications and their limits**

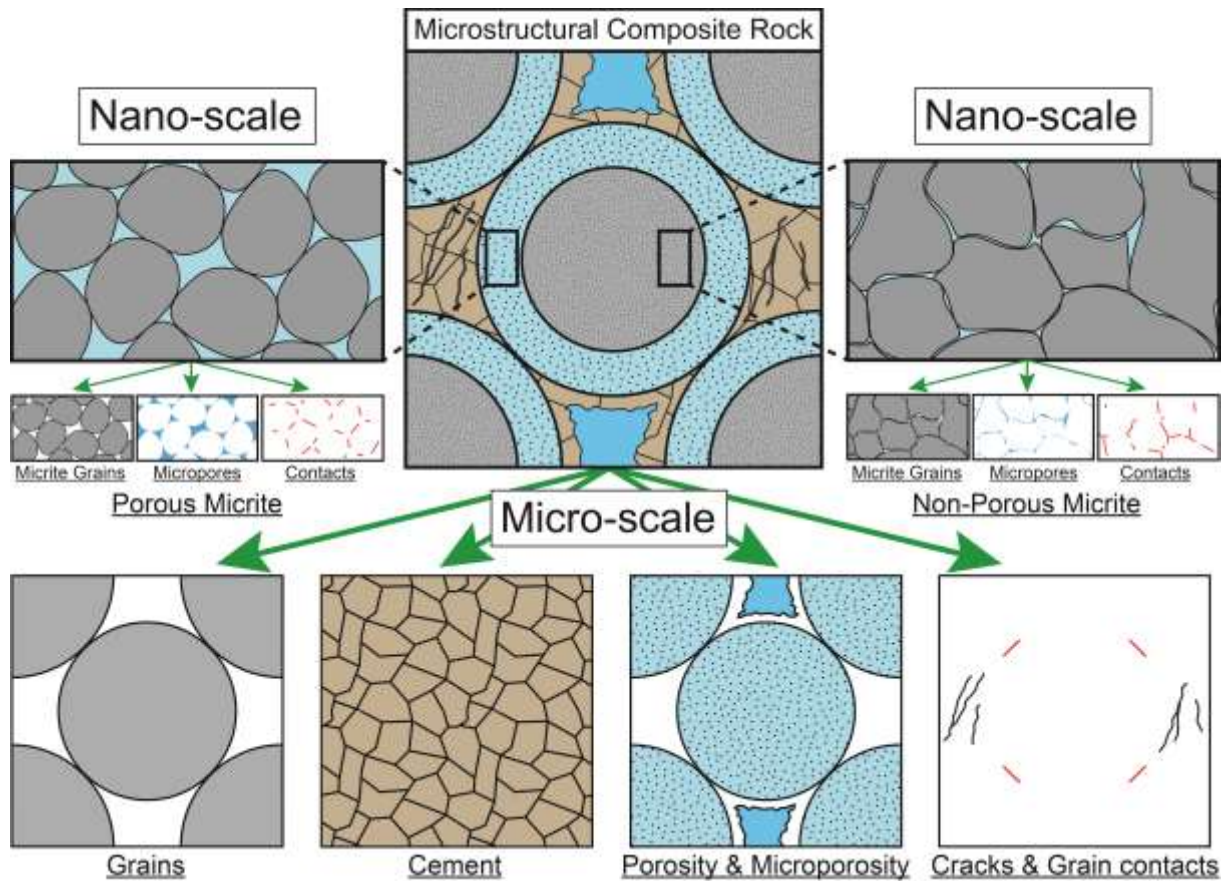
5 The solid structure (grains, matrix) is usually characterized using the Dunham carbonate rock
6 classification (Dunham, 1962). It was originally developed for sedimentology studies of carbonate
7 rock reservoirs, and its approach to define carbonate constituents is mostly descriptive. The reason for
8 this terminology to be widely used in carbonate rock physics is because it gives a quick overview of
9 some crucial parameters controlling the response of some physical properties: the nature of “grains”
10 (ooids, bioclasts...), their relative amount and their distribution in space (grain to grain contacts *versus*
11 grain spreading), and the nature of the matrix (cements, micritic-mud matrix...).

12 Another crucial feature for rock physical properties in carbonates is the porosity. Porosity description
13 and characterization is a very difficult exercise to do, because of the tremendous heterogeneity of pore
14 size and shape. One of the oldest classifications to date is that of Choquette and Pray (1970), which is
15 still used nowadays in some cases. Here, the distinction is made between “fabric selective” and “non-
16 fabric selective” porosity and thus is strongly linked to the rock texture. This classification is pretty
17 hard to use in rock physics because it gathers under the same category some pore types that have a
18 complete different influence on physical properties. It also becomes quickly limited because there are
19 often no obvious and systematic relationships between initial rock textures and the porosity evolution
20 through time (Lucia, 2007). This led to more rock-physics oriented classifications that emerged in the
21 beginning of the 2000’s, with Lønøy (2006) and Lucia (2007). Both classifications are widely used in
22 carbonate reservoir characterization and reservoir engineering. They try to integrate transport
23 properties at different scale using a large number of pore type, characterized by their size, shape and
24 connectivity. Although those new “petrophysical” classifications fill some gaps left by the old ones,
25 they are still not optimal, because rock physic relationships in carbonate rocks are often poorly-
26 defined.

27 The size, shape, density and spatial arrangement of pores and grains, the nature of the phase (cement
28 *versus* matrix), alongside with natural fractures and cracks, define a microstructural pattern (although

1 some of those microstructures are certainly not exclusive to carbonate rocks) (figure 1). The coupled
2 effect between all those features are known to have a great influence on rock physical properties, and
3 deciphering the signal or attributing an effect to one parameter is not that simple.

4



5

6 Figure 1: Microstructural features and pattern in carbonate rocks at micro and nano-scale.

7

8 Fortunately, the rock physics properties measured at the macroscopic scale are often sensitive to small
9 variations of the solid and pore structure. From this observation, some physical parameters are thus
10 highly valued, because they can bear most of the microstructural information. This information can be
11 obtained from the seismic properties of the rocks and their transport properties. In general, the seismic
12 properties (P & S-wave velocities, velocity dispersion and attenuation...) are largely controlled by the
13 contacts between the rock components, while the transport properties (permeability, electrical
14 conductivity...) are more sensitive to pore geometry and the overall pore throat network architecture
15 (connectivity, tortuosity).

1

2 **3. Microstructures and elastic properties**

3 The development of sequential stratigraphy and the revival for oil exploration in the 70's and 90's,
4 made many geological investigations possible from drilling and geophysical measurements. Given the
5 importance taken by the subsurface exploration and investigation, understanding the elastic properties
6 of rocks is essential to the interpretation of seismic reflectors, logs, and velocity data measured in the
7 laboratory. Seismic waves are, by nature, small mechanical perturbations of the medium. They are
8 therefore logically affected by the microstructures of the rock and by deformation processes.
9 Laboratory measurements using elastic waves are particularly interesting because the processes
10 involved in ultrasonic wave propagation are similar to those of seismic exploration. Only the
11 frequency domain changes (50 Hz in seismic, 10 kHz in logging, and 1 MHz in laboratory methods)
12 making the wavelengths and the investigated volumes very different. Those three methods are
13 therefore not sensitive to the same heterogeneities and the extrapolation from the field to the
14 laboratory data becomes a delicate issue. This section is focused on the frequency domains of the
15 logging (sonic) tools and the laboratory (ultrasonic) methods.

16

17 **3.1 Porosity**

18 Porosity is the first order parameter controlling elastic wave velocities in sedimentary rocks: as
19 porosity increases, the P and S-wave velocities decrease (Mavko et al. 2009). This relationship is
20 rarely strictly linear, but rather describes a concave upward evolution, as shown in figure 2, modified
21 from Verwer et al. (2008). This type of graph where $V_p = f(\text{porosity})$, highlights the large velocity
22 dispersion at a given porosity, which is attributed to the microstructural parameter. Here, RHG and
23 WTA stand for Raymer-Hunt-Gardner and Wyllie's Time Average equations. Those two expressions
24 that relate velocity to porosity and to pore-fluid compressibility are among the most popular porosity-
25 to-velocity transform in rock physics. Such relations are often used as additional controls for inferring
26 porosity from well logs, as well as in-situ indicators of pore fluid type. The oldest and most popular is
27 the Wyllie et al. (1956) equation:

1
$$\frac{1}{V_p} = \frac{1-\phi}{V_m} + \frac{\phi}{V_f}. \quad (1)$$

2

3 where ϕ is porosity, V_p is the measured P-wave velocity, and V_m and V_f are the P-wave velocities in
4 the solid (matrix) and in the pore-fluid phases, respectively.

5 The RHG equation (Raymer et al., 1980) is another widely used porosity-to-velocity transformation
6 (here, for $\phi < 37\%$):

7
$$V_p = (1-\phi)^2 V_m + \phi V_f. \quad (2)$$

8

9 And for $\phi > 47\%$:

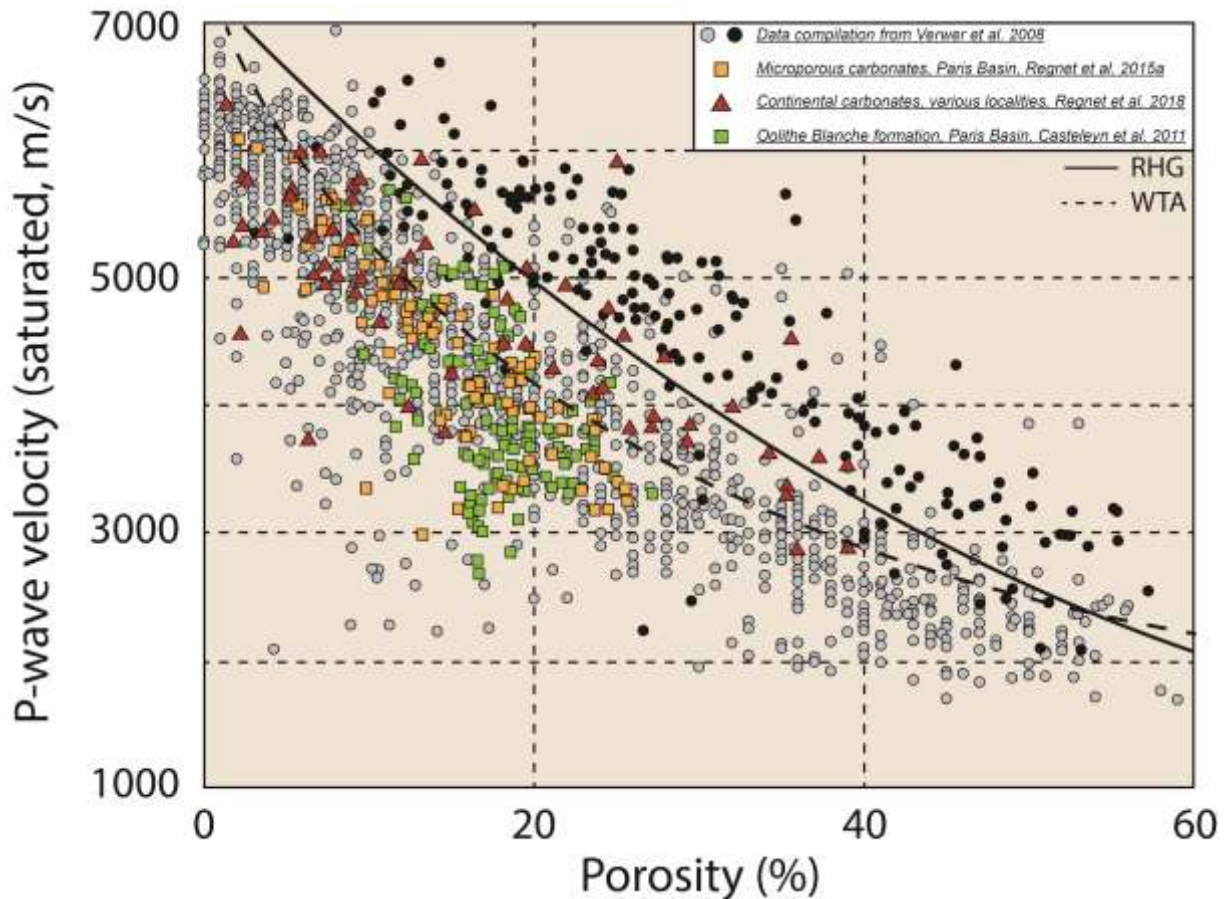
10
$$\frac{1}{\rho V_p^2} = \frac{\phi}{\rho V_f^2} + \frac{1-\phi}{\rho V_m^2}. \quad (3)$$

11

12 Those expressions present a handy, but deceitful form of summarizing extensive experimental data.
13 Indeed, there is no physical reason for the total travel time of a wave in a two-component medium to
14 be the sum of the travel times in the individual components (unless the two components are arranged
15 in layers normal to the direction of wave propagation, and the wavelength is small as compared to the
16 thickness of an individual layer). Following those empirical and non-physical time average equations,
17 more meticulous and physics-oriented models emerged in the early 80's. They mostly provide
18 relations among velocity, porosity, and pore-fluid compressibility. Such relations take into account the
19 internal structure of rocks. Examples of effective medium models are: Hudson (1990), for cracked
20 rocks; Kuster and Toksöz (1974), for low-porosity rocks; Berryman (1980), for low-to medium-
21 porosity rocks; Digby (1981), Walton (1987), and Dvorkin et al. (1994) for high-porosity granular
22 rocks. Reviews of such theories are given by Zimmerman (1991) and Wang and Nur (1992), and
23 compiled in a convenient way in Mavko et al. (2009).

1 The data scattering observed in figure 2 can be the “acoustic signature” of the different pore
2 geometries (equant or compressible porosity), and to a lesser extent of the saturating fluids
3 (considering the case of sonic logs).

4



5

6 Figure 2: P-wave velocity evolution with porosity (saturated conditions) over a large data set (grey and
7 black dots are taken from the original compilation by Verwer et al. (2008), modified). RHG
8 and WTA stand for the Raymer-Hunt-Gardner's and Wyllie's Time Average trends.

9

10 A summary of the theoretical effect of each pore geometry according to the definition of Choquette
11 and Pray (1970) was proposed by Wang (1997). In practice, highlighting the effect of a pore geometry
12 on the P or S-wave velocities is not an easy work, as the simultaneous occurrence of several
13 geometries within the same rock is very common. Eberli et al. (2003) and the integrated study of the
14 ODP-133 well of the Great Bahama Bank of the Caribbean remains to this day a reference. These
15 carbonate formations are young (Miocene-Pliocene), and have undergone a reduced diagenesis, so the
16 primary porosity and its geometry is relatively well preserved and very similar from pore to pore.

1 Eberli et al. (2003) recognize the effect of five categories of pores (*sensu* Lucia (1983, 1995, & 1999))
2 (figure 3):

3

4 - Cemented limestones are characterized by high P-wave velocities because of the porosity reduction
5 induced by cementation processes. At porosity close to zero, we almost reach velocity values of the
6 calcite ($V_p = 6000$ m/s; $K = 70$ GPa) and the dolomite ($V_p = 6500$ m/s; $K = 80$ GPa, values from
7 Mavko et al., 2009).

8

9 - The interparticle and intercrystalline porosities cannot be discerned on the simple basis of P-wave
10 velocities. In both case, the sedimentary fabric (rock fabric) consists of an assembly of elements with
11 very little amount of cement or matrix. This poorly cohesive accumulation of grains or crystals is
12 characterized by relatively low P-wave velocities at a given porosity.

13

14 - The moldic porosity develops during the early stages of diagenesis by simple preferential dissolution
15 of aragonitic grains (a metastable carbonate phase). This dissolution creates a very dense and
16 continuous sparitic network that favors wave propagation. Thus, carbonate rocks with 50% of moldic
17 porosity can have velocities between 4000 m/s and 5000 m/s which are abnormally high for such
18 porosity values, especially when the moldic pores are large. Acoustic wave velocities of rocks with
19 small moldic pores will be well predicted by Wyllie's (1956) time-averaging equations. The difference
20 of size between the moldic pores is therefore reflected in a very strong dispersion of velocity values.

21

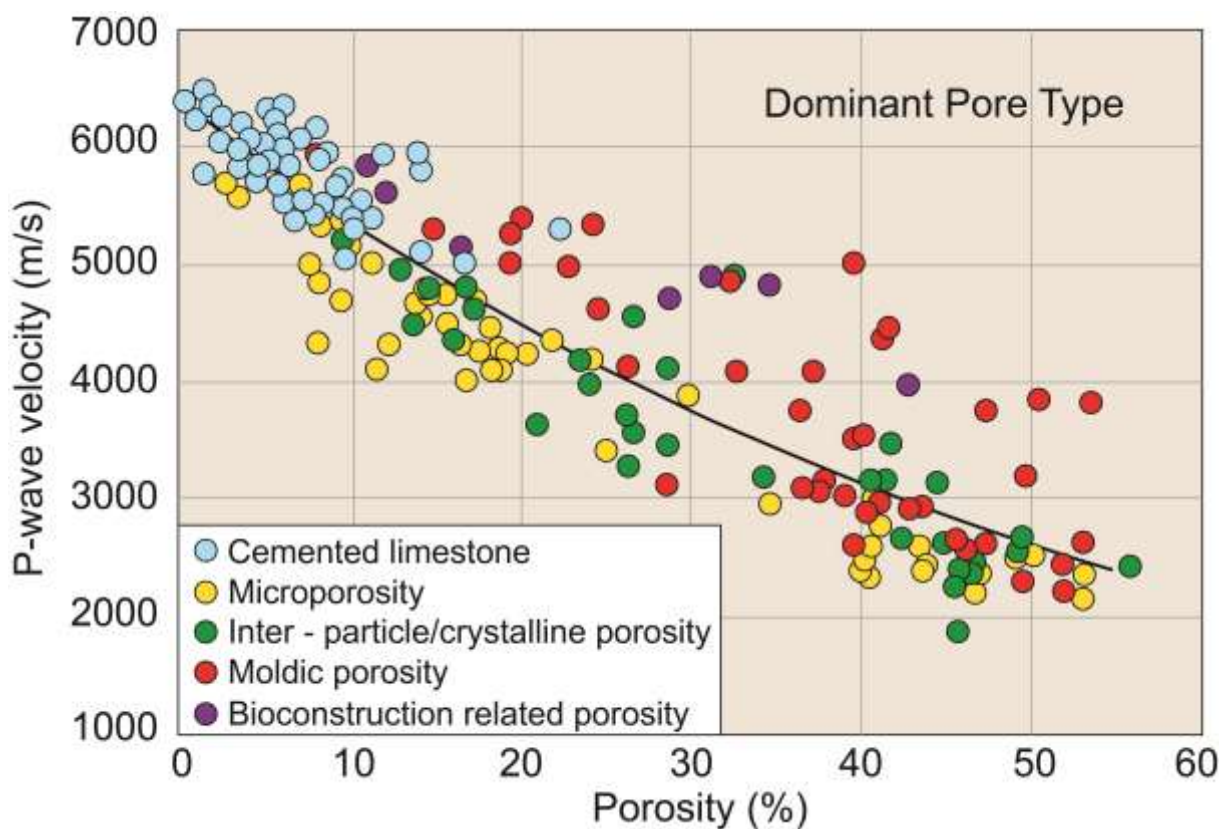
22 - The bioconstruction related porosity is the porosity created during the growth of organic individuals
23 (intraframe porosity or growth framework porosity) is usually found in the framestone and boundstone
24 carbonate textures. These pores are therefore included in a crystalline and continuous structure, and
25 have an acoustic signature very similar to large molded pores.

26

27 - The microporosity concerns pores smaller than $10\ \mu\text{m}$ (*sensu* Lønøy (2006)) and seems to follow the
28 same trends as the interparticle and intercrystalline porosities, with relatively low velocities compared

1 to other geometries of pores. Those micropores rely on the morphology and size of the micrite
2 particles (microcrystalline calcite, Folk 1966). The effect of such structures on the acoustic properties
3 of carbonates is poorly documented, except for some studies on chalk formations in the North Sea
4 (Japsen et al. 2004; Røgen et al. 2005; Fabricius et al. 2007; Gommesen et al. 2007), on micritic facies
5 of the Urgonian formation (Lower Cretaceous) of southern France (Fournier & Borgomano 2009), and
6 on the recent work of Casteleyn et al. (2010, 2011) and Regnet et al. (2015a, 2015b) developed at the
7 University of Cergy-Pontoise (see section 5 for details).

8



9

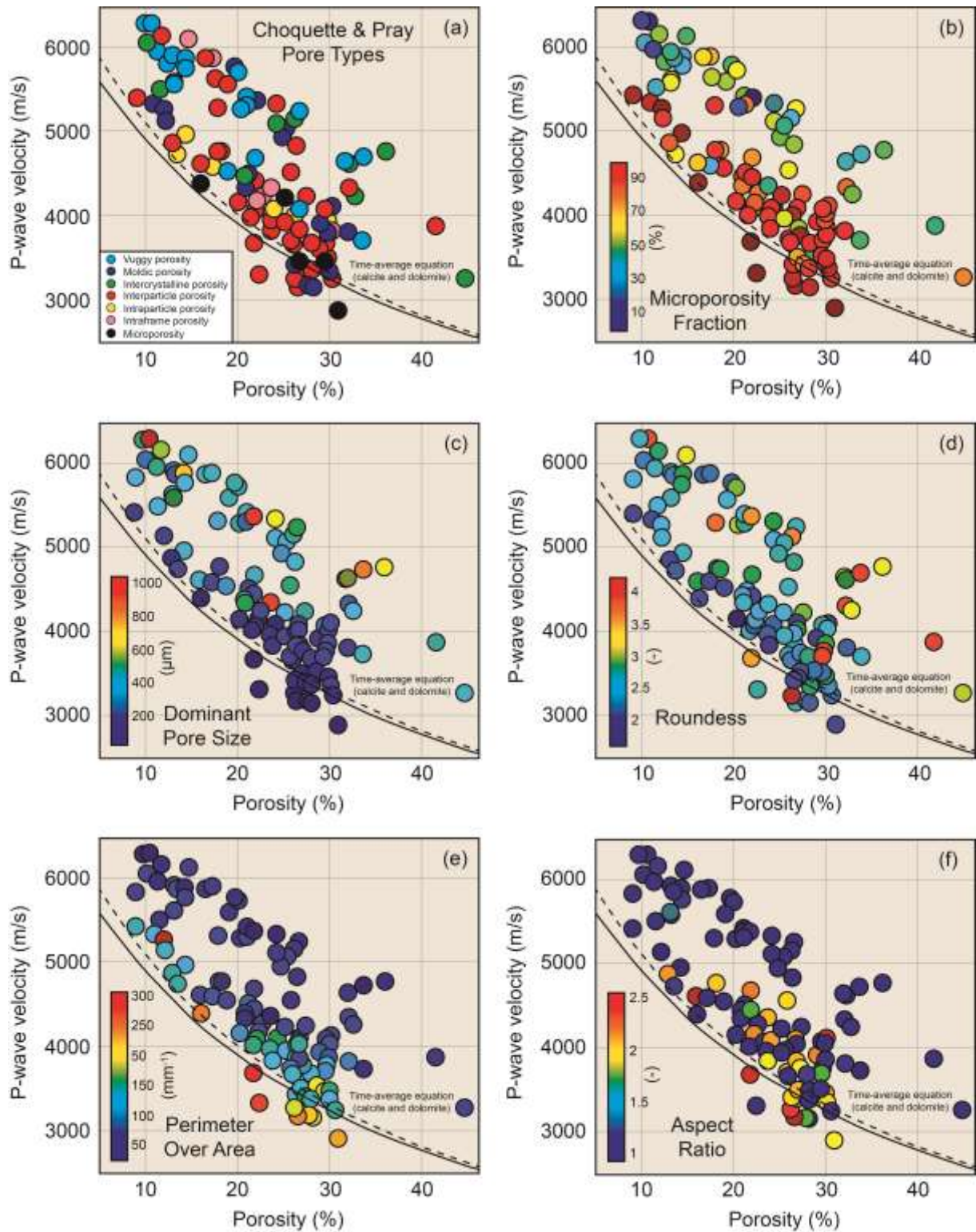
10 Figure 3: P-wave velocity evolution with porosity. Data points are discriminated by the dominant pore
11 type. The black line is the average trend (exponential best fit curve) for all data points.
12 Samples are from the ODP Site 1003 of the Great Bahama Bank. After Eberli et al. (2003),
13 modified.

14

15 Those five types of pores and their effects on acoustic properties come from the classifications
16 previously presented and are used to link and understand the porosity-velocity relationship. They
17 remain nevertheless very descriptive, and therefore very limited. They do not represent any
18 quantitative geometric factor, to which the propagation of P-waves would be sensitive to.

1 Weger et al. (2009) proposed a quantitative approach based on image analysis techniques from which
2 several 2D parameters are extracted, such as size, roundness, aspect ratio, and PoA (Perimeter over
3 Area) which is the ratio between the total perimeter that encloses the pore space and the total pore
4 space area on a thin section. It can be regarded as a two-dimensional equivalent to the specific surface
5 area that is defined as the ratio between pore volume and pore surface (Kozeny, 1927). Generally, a
6 small number indicates a simple geometry and a large number an intricate pore system.

7 In addition, the dominant pore size, the pore aspect ratio and the microporosity fraction, seem to also
8 have a great impact on the P-wave velocity. It is very common to find associated macroporosity and
9 microporosity within the same rock. Pores smaller than $10\mu\text{m}$ (*sensu* Lønøy (2006)) are considered to
10 be part of the microporosity. Those elements convey the general idea that a rock with a large specific
11 surface area, a great amount of micropores and/or low pore aspect ratio is a more compressible
12 medium that limits wave propagation. In this case, it is the macro/microporosity ratio that will be the
13 controlling parameter. Those settings are all highly significant and explain the relations between
14 porosity geometry and P-waves fairly well (figure 4). On the other hand, the pore geometries defined
15 by Choquette and Pray (1970) and the roundness parameter are here ineffective and fail to explain the
16 observed porosity-velocity relationship.



1

2 Figure 4: P-wave velocity evolution with porosity. Data points are discriminated by: (a) the dominant
 3 pore type from the Choquette and Pray (1970) classification, (b) Microporosity fraction, (c)
 4 Dominant pore size, (d) Pore roundness, (e) Perimeter over area of pores, (f) Pore aspect
 5 ratios. Samples are from the Shu'aiba Formation (Middle East) and are Aptian in age, from an
 6 isolated platform of Miocene age in Southeast Asian, and from two drowned platforms on the
 7 Marion Plateau (Australia) and are also Miocene in age. After Weger et al., 2009, modified.

8

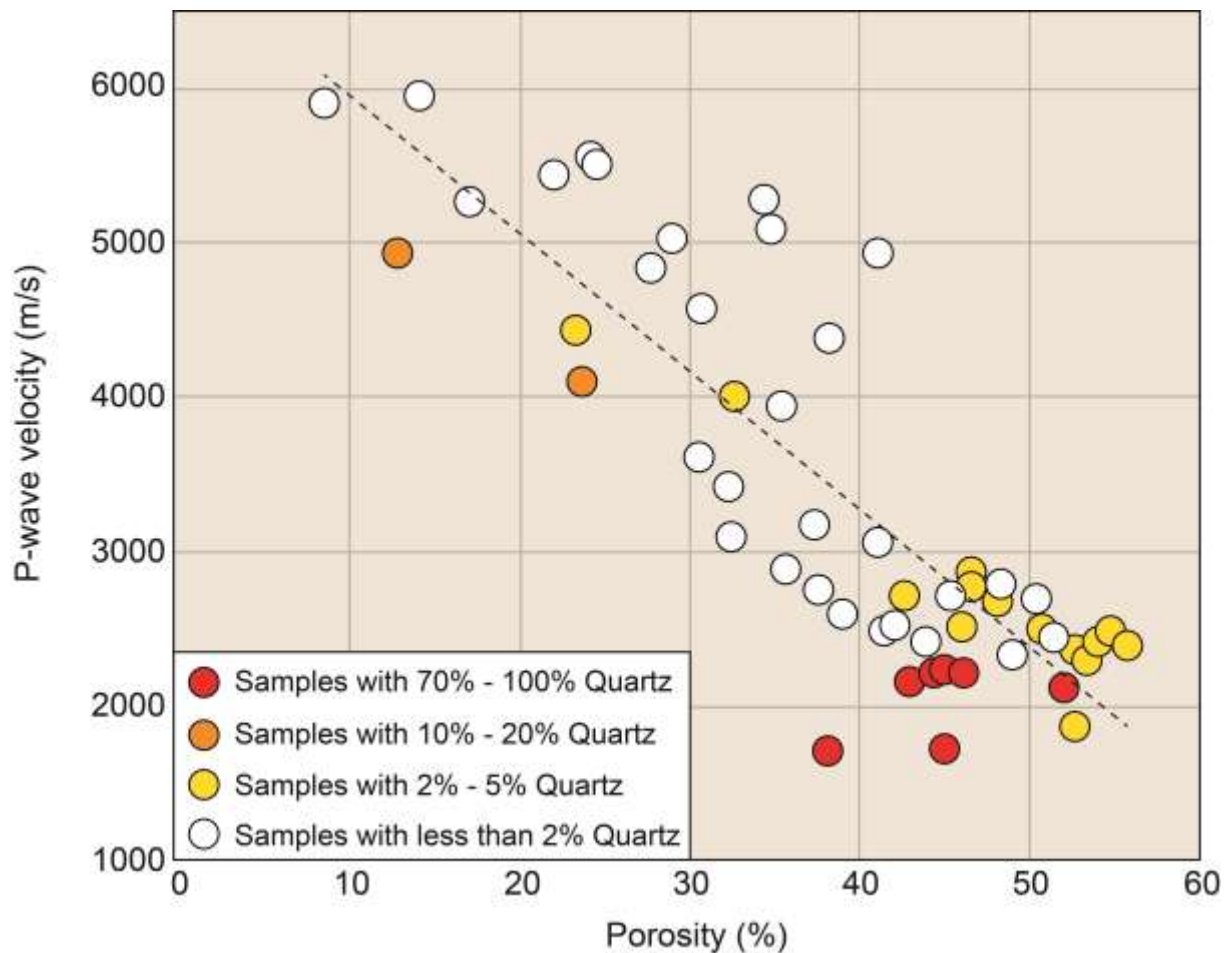
1

2 Other pore types and their effects on wave propagation are not studied in depth because the
3 observation scale of those pores often exceeds the size of the samples used for laboratory
4 measurements. This is particularly the case of channel, vuggy and fracture porosity (according to
5 Choquette and Pray (1970)) whose effects are mainly observed at the multi-decimetric or metric scale.

6

7 **3.2 Mineralogy**

8 Mineralogical composition is a determining factor with respect to P and S-wave velocities. Carbonate
9 rocks may display complex mineral compositions. Calcium carbonate [CaCO₃], which is the main
10 mineral, is often associated with minerals of detrital origin such as clays (marls and argillaceous
11 limestones), quartz/feldspar (calcarenite), or other minerals drained from continental sources during
12 alteration, especially when considering continental carbonate rock systems. The seminal works of
13 Rafavich et al. (1984), followed by Eberli et al. (1993), Anselmetti et al. (1997) and more recently the
14 compilation of Kenter et al. (2007) highlight that the proportions of those minerals in carbonate rocks
15 have a strong influence on the P and S-wave velocities, because they are all characterized by different
16 elastic bulk moduli K (calcite 63.7 GPa to 76.8 GPa, dolomite 76.4 GPa to 94.9 GPa, kaolinite 1.5
17 GPa, quartz 36.5 GPa to 37.9 GPa, feldspar 37.5 GPa to 75.6 GPa (albite), see Mavko et al. 2009 for
18 more details). For example, when the proportion of quartz is lower than 5%, the effect on P and S
19 wave velocities is almost zero (figure 5).



1

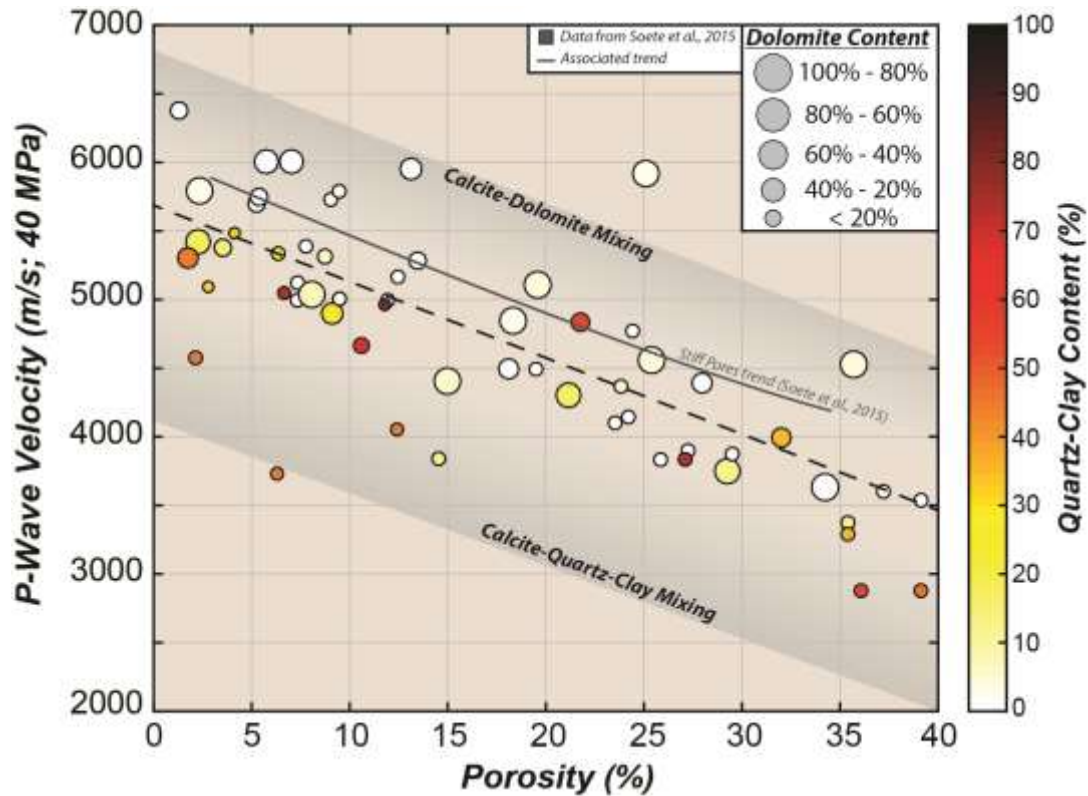
2 Figure 5: P-wave velocity evolution with porosity. Data points are discriminated by quartz fraction
 3 within the sample. Samples with high quartz fraction display lower velocities at a given
 4 porosity. Samples are from the Florida Keys formation (subsurface). After Anselmetti et al.,
 5 1997, modified.
 6

7 Beyond this threshold those minerals (quartz, clays) will gradually reduce the acoustic wave velocities
 8 as well as the associated dispersion. It usually results in a much more linear porosity-velocity trend.

9 This is also shown in continental carbonates (figure 6, Regnet et al., 2018), where we can also observe
 10 the duplicity of dolomite when it comes to the elastic properties: the difference between the elastic
 11 properties of calcite and dolomite is high enough so that, similar to siliciclastic rocks, some control of
 12 the dolomite on the wave velocity of carbonate rocks might be expected. On the contrary, in this case
 13 we observe that dolomitized samples are not only found in the higher trend as one should expect, but
 14 they are also centered in the average trend of the data set (figure 6). This shows that the effect of
 15 dolomitization on the elastic properties is much more diluted because the associated features of
 16 dolomitization also strongly modify the existing pore geometry and the total porosity as well

1 (Anselmetti et al., 1997; Eberli et al., 2003; Regnet et al., 2018). Acoustic waves are then much more
2 dependent on the pore type inherited from the dolomitization processes, which will change in a more
3 or less important way the shape of the pores, and thus their compressibility.

4



5

6 Figure 6: P-wave velocity evolution through porosity variation. Data points are discriminated with
7 their quartz/clay content (dot color, associated with the side colorbar) and with their dolomite
8 content (dot size). Two mineralogical domains are individualized (calcite-dolomite mixing and
9 calcite-quartz mixing zones). Evolution trend collected from Soete et al. (2015) showing the
10 velocity-porosity relationship where stiff pore inclusions are dominant is also reported in the
11 figure. After Regnet et al., 2018.

12

13 Kenter et al. (2007) highlights on a very broad dataset a threshold value of proportion in carbonate
14 (22%) and clay (8%) above which the propagation speeds of the P waves are respectively high and
15 low. This effect is even more noticeable if the porosity is low.

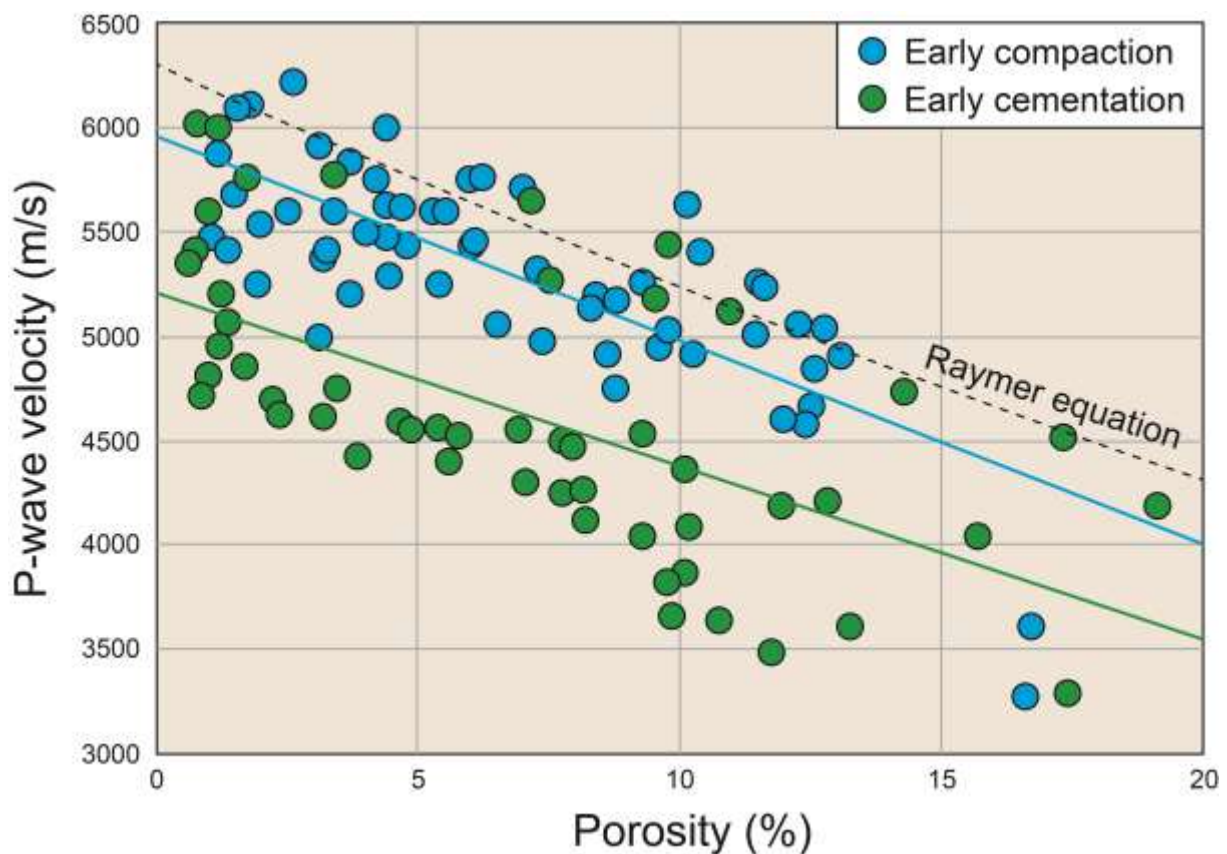
16

17 3.3 Cements and crystalline phases

18 Cements can be very abundant in sedimentary rocks. They are usually responsible for the larger
19 decrease in the total porosity of carbonate rocks. Those cements are known as “blocky cements”

1 (Brigaud et al., 2010). By decreasing the amount of voids, cements make the rock more cohesive, stiff
2 and create a continuous medium that facilitates the wave propagation. All types of sparitic cement
3 (inter-intraparticulate, syntactic...) have a similar seismic signature, with the exception of isopachous
4 cements (Brigaud et al., 2010) that are abundantly found in granular carbonates (grainstones,
5 rudstone...). These isopachous cements appear in the early stages of carbonate rock diagenesis, and
6 are generally markers of shallow depositional environments, such as a shoreface or an oolitic shoal.
7 Those cements are very important for the evolution of rock frame, because they reduce mechanical
8 compaction. They result in a heterogeneous medium where grains are unconnected and delimited by
9 this early cement. This additional mechanical interface between grains seems to induce diffraction
10 phenomena of elastic waves, thus explaining the scatter of P-wave velocities (figure 7).

11



12

13 Figure 7: Influence of early cements (isopachous fringes) on the P-wave velocity evolution with
14 porosity, Middle Jurassic Limestones from the Paris Basin. The early cementation of
15 grainstones prevents the formation of a continuous medium, favoring wave scattering and
16 refraction during the wave propagation. After Brigaud et al. (2010), modified.

17

1 Conversely, grainstones that have undergone a strong physicochemical compaction, due to the absence
2 of early cementation, display a good network between the constitutive elements (grains and cements)
3 forming a homogeneous physical environment that favors acoustic wave propagation. With that in
4 mind, one can interpret the porosity-velocity trend in terms of diagenetic evolution where oolitic sand
5 can follow two paths during its history. In the case of early cementation and subsequent filling of the
6 porosity with blocking cements, the P-wave velocities will be relatively low at a given porosity.

7

8 **4. Microstructures and transport properties**

9 On larger scales, petroleum systems, hydrothermal, geothermal energy, mineral deposits and
10 underground storage are all domains where transport properties play a decisive role. At the laboratory
11 scale, the characterization of reservoir properties essentially relies on permeability and electrical
12 conductivity measurements. The latter is also widely used as a logging tool. Those two physical
13 parameters are representative of the porous network in terms of geometry, pore connectivity, and
14 microstructure.

15 Permeability is a transport property that measures the capacity and efficiency of a fluid to percolate
16 through a porous medium. Permeability is estimated from Darcy's law (Darcy 1856).

17 Electrical conductivity is very complementary to permeability. Differences in conductivity between
18 the minerals in a rock are, in most cases, quite irrelevant compared to the contrast between mineral
19 conductivity and the one of the fluid saturating the pore space (usually brine). The electrical current
20 essentially "flows" in pores saturated with brine, and this flow-path is imposed by the microstructure.

21 A saturated rock can reasonably be considered as a two-phase medium: solid grains and brine. The
22 conductivity ratio of these two phases (σ_m and σ_e) is so small (10^{-10}) that minerals can be seen as non-
23 conductive (with the exception of iron-rich minerals and clays). The effective conductivity σ_{eff} of a
24 rock is therefore proportional to the conductivity of the electrolyte σ_e :

$$25 \quad \sigma_{eff} = \frac{\sigma_e}{F} + \sigma_s. \quad (4)$$

26

1 where F is the formation factor and σ_s the surface conductivity, which represents the conductivity
2 located in the immediate vicinity of the minerals, in the so-called electrical double layer adsorbed at
3 the mineral surfaces (Guéguen and Palciauskas, 1994). Since the ratio σ_m and σ_e is close to zero (10^{-10}),
4 F mainly depends on the microstructure. The formation factor F and the tortuosity τ are two quantities
5 calculated from electrical conductivity measurements that characterize the porous medium in a precise
6 way:

$$7 \quad F = \frac{\tau}{\phi}. \quad (5)$$

8
9 where ϕ is the porosity. The formation factor F can be seen as the reduction factor by which the
10 conductivity of the solution is affected by the insulating phase (grains, cement or matrix). The
11 tortuosity coefficient accounts for the imperfect connectivity of the medium and describes the tortuous
12 path followed by the electric current. A high tortuosity indicates a low connectivity of the porous
13 network. When detailed information on the porous network is missing, the use of empirical
14 relationships is very often required. Archie's law (Archie, 1942), which relates the porosity ϕ to the
15 formation factor F for a totally saturated rock, is probably one of the most used relation:

$$16 \quad F = \phi^{-m}. \quad (6)$$

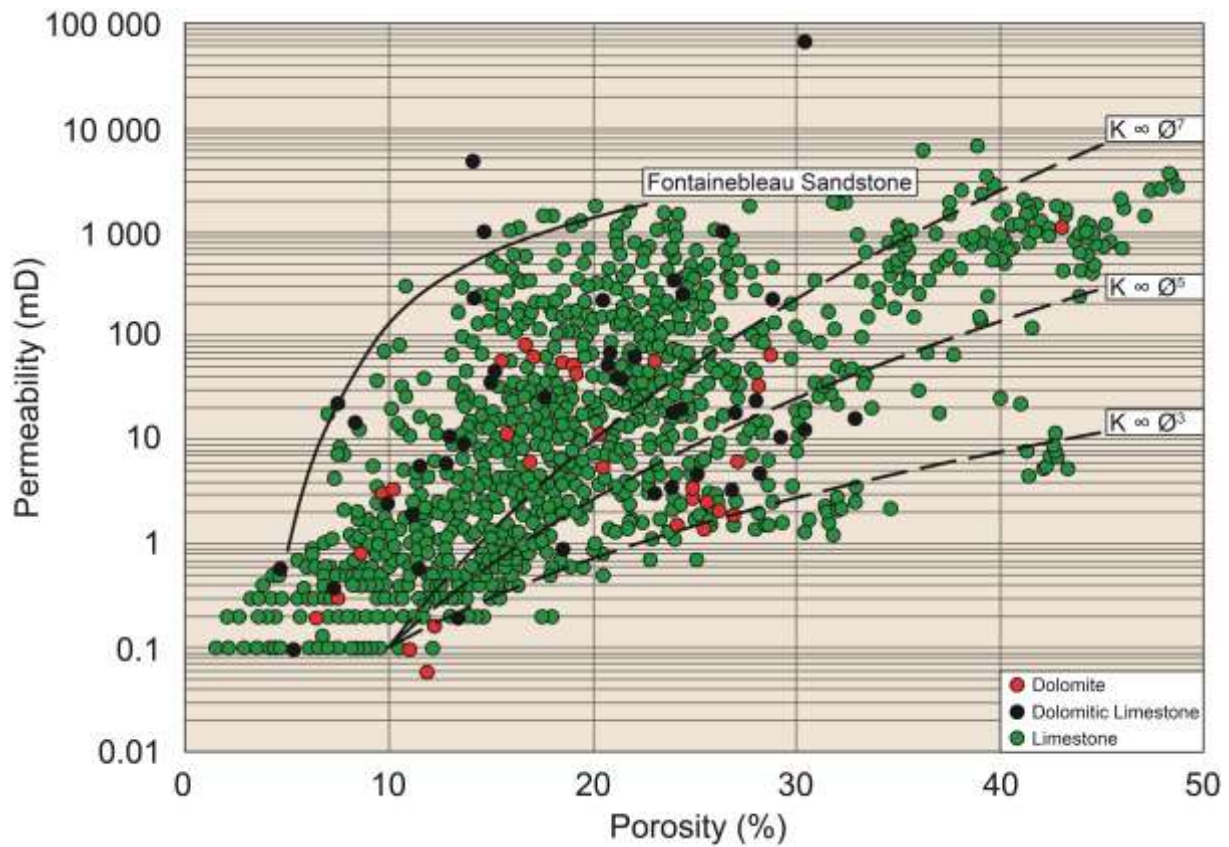
17
18 where m is the cementation exponent, a parameter with no real petrographic value. It mainly represents
19 and accounts for the overall cohesion of a rock and can characterize a sedimentary lithology or a
20 particular microstructure. It is noteworthy that there is no theoretical reason for this relationship to be
21 valid for all microstructures whatever the porosity value might be, as it is an empirical relationship
22 developed for clean sandstones.

23

24 **4.1 Porosity**

25 Although no simple relationship exists between porosity and permeability, the investigation and
26 definition of such correlations is paramount in rock physics. In carbonate rocks, the porosity-

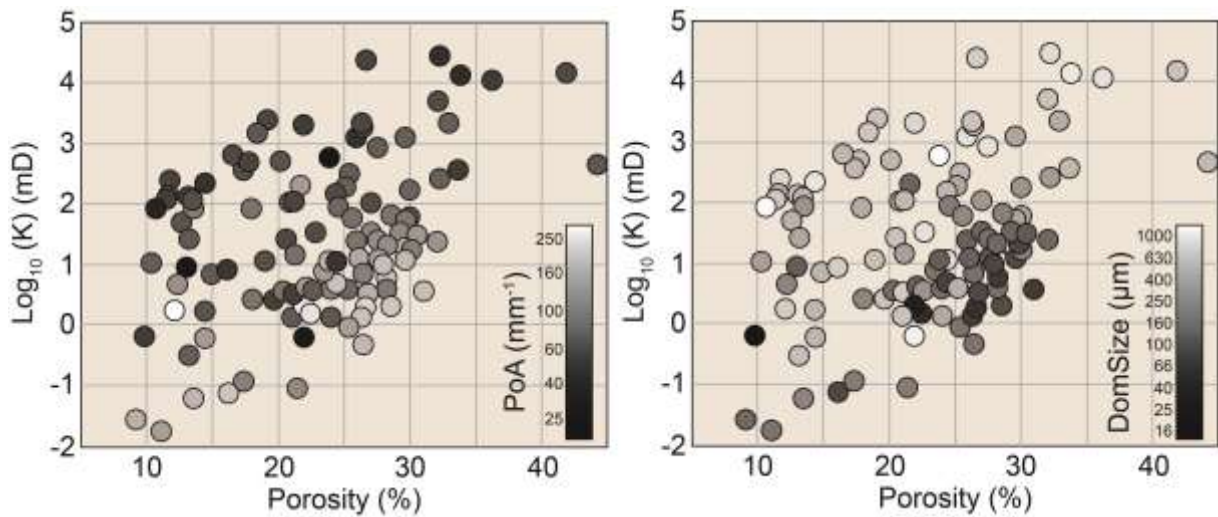
- 1 permeability relationships are poorly defined (and poorly documented for some particular carbonate
- 2 lithologies) and highly scattered, especially on large datasets (Zinszner & Pellerin, 2007) (figure 8).



3
 4 Figure 8: Porosity-permeability evolution of carbonate rocks on a large data set. Several power-laws
 5 are represented on the graph, alongside with the porosity-permeability relationship for the
 6 Fontainebleau Sandstones. After Zinszner and Pellerin (2007), modified.
 7

8 This dataset shows porosity-permeability values for various carbonate rocks and sandstones, which
 9 lies between two extreme behaviors. The higher values coincide with the correlation found for the
 10 Fontainebleau sandstones (Bourbié and Zinszner, 1985), whose values are rarely reached in the
 11 carbonates. The lower values are typical of fine carbonate textures like mudstones. But more than the
 12 texture itself, the main reason for this dispersion is the large variability of pore geometry and the
 13 connectivity of the porous network. As previously presented, Choquette and Pray classifications
 14 (1970) and the more successful ones of Lucia (1983, 1995, 1999 & 2007) or Lønøy (2006) have a
 15 limited use and fail to explain the porosity-permeability trends observed in carbonates. When taking
 16 into account data from pore space quantifications derived from image analysis techniques and
 17 developed by Weger et al. (2009), pore geometry appears to be predominant, especially when

1 considering pore size and the complexity of the porous network through the PoA (figure 9). Samples
2 characterized by low permeability for a given porosity have high values of PoA (which represents a
3 complex porous medium with a large surface area) and small pore sizes. Those observations are made
4 on digital image analysis, but pore space geometry can also be assessed through laboratory
5 measurements provided by mercury injection capillary pressure (MICP) methods.

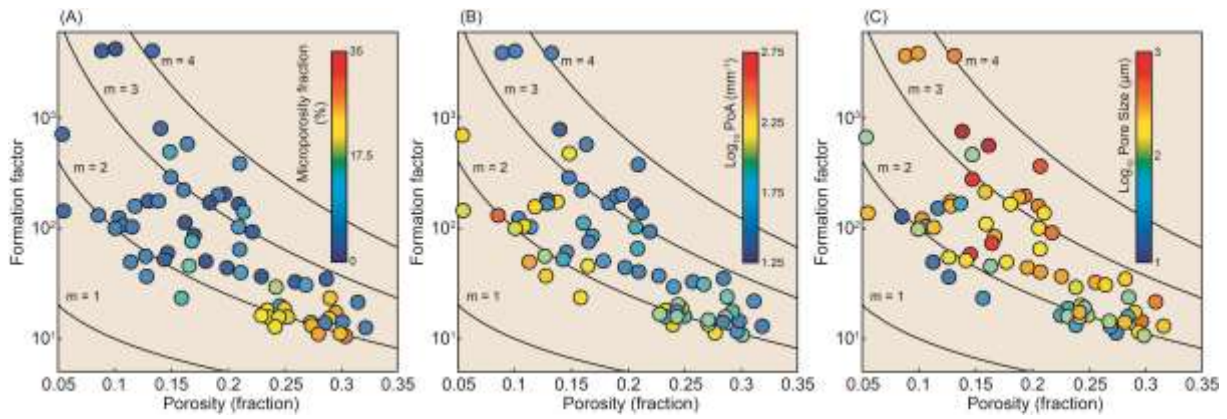


6

7 Figure 9: Porosity-permeability evolution of carbonate rocks regarding the influence of the Perimeter
8 Over Area (PoA) of the pores, and the dominant pore size (DomSize). Samples are from the
9 Shu'aiba Formation (Middle East) and are Aptian in age, from an isolated platform of
10 Miocene age in Southeast Asian, and from two drowned platforms on the Marion Plateau
11 (Australia) and are also Miocene in age. After Weger et al. (2009), modified.
12

13 4.2 Electrical conductivity

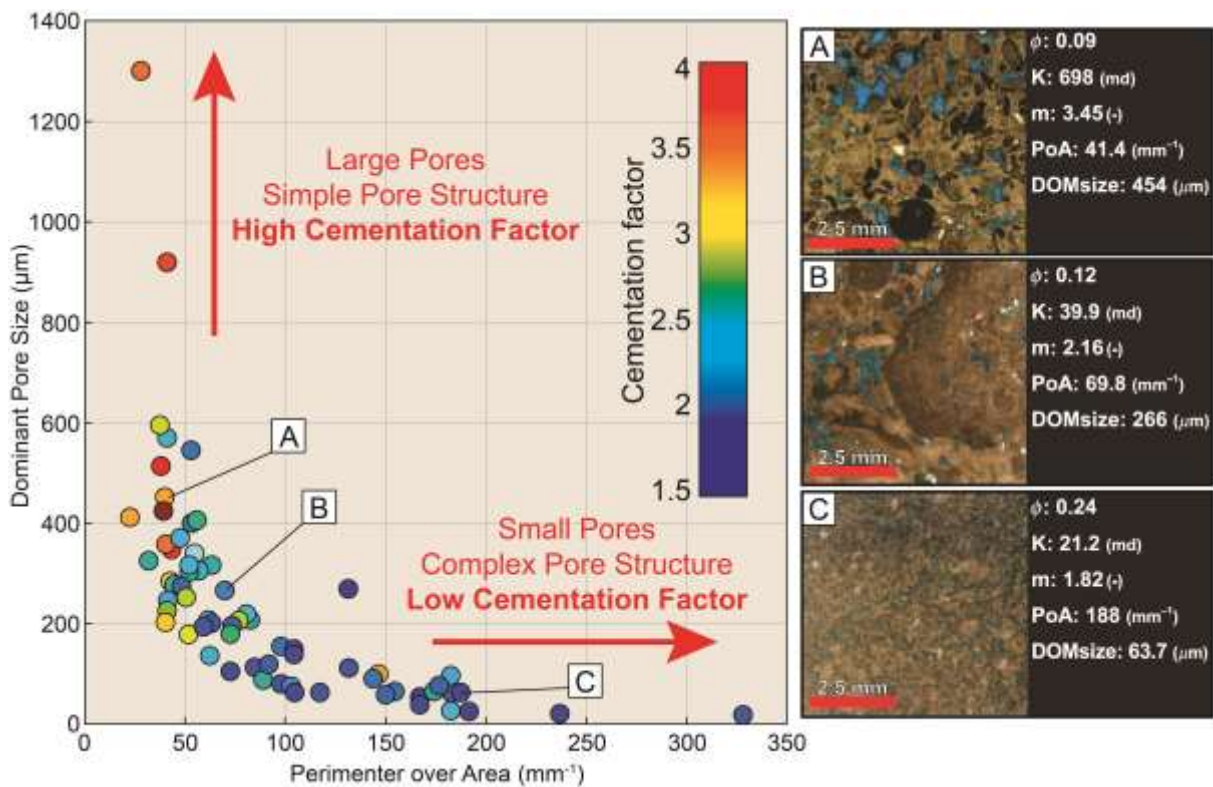
14 Porosity and formation factor relationships are at least as complex as those observed for porosity and
15 permeability. The work of Verwer et al. (2011), based on the image analysis method developed by
16 Weger et al. (2009) presented in the previous sections, shows that the "flow" of electrical current is
17 controlled by the combined effect of pore sizes, the proportion of microporosity and the complexity of
18 the porous network (figure 10). The cementation exponent can be related to the dominant pore size and
19 PoA. A rock with small pore sizes and an intricate porous network (high PoA) will be characterized by
20 a low cementation exponent, while a rock with large pores and a relatively simple pore network will
21 be characterized by high cementation exponent. This is somehow paradoxal because when linking the
22 law depending on tortuosity (eq. 5) to Archie's law (eq. 6), a high cementation exponent correlates to a
23 strong tortuosity, which is not consistent with a simple pore network as shown on figure 11.



1

2 Figure 10: Formation factor evolution with porosity. Data points are discriminated by: (a)
 3 Microporosity fraction, (b) Perimeter over Area and (c) Dominant pore size. Black lines show
 4 the value of the cementation exponent, using equation (6). Samples are from the Khuff and the
 5 Shu'aiba formations (Middle East) and are Permian and Cretaceous in age, respectively; from
 6 two drowned platforms on the Marion Plateau (Australia) and are Miocene in age; from the
 7 Maiella Mountain (Italy) and are Cretaceous in age. The samples from the Bahamas were
 8 taken from a Holocene stromatolite. After Verwer et al. (2011), modified.

9



10

11 Figure 11: Dominant Pore Size and Perimeter over Area evolution in carbonate rocks. Data points are
 12 characterized by the value of the cementation factor and highlight two domains of porous
 13 structures and networks. Samples are from the Khuff and the Shu'aiba formations (Middle
 14 East) and are Permian and Cretaceous in age, respectively; from two drowned platforms on the
 15 Marion Plateau (Australia) and are Miocene in age; from the Maiella Mountain (Italy) and are
 16 Cretaceous in age. The samples from the Bahamas were taken from a Holocene stromatolite.
 17 After Verwer et al. (2011), modified.

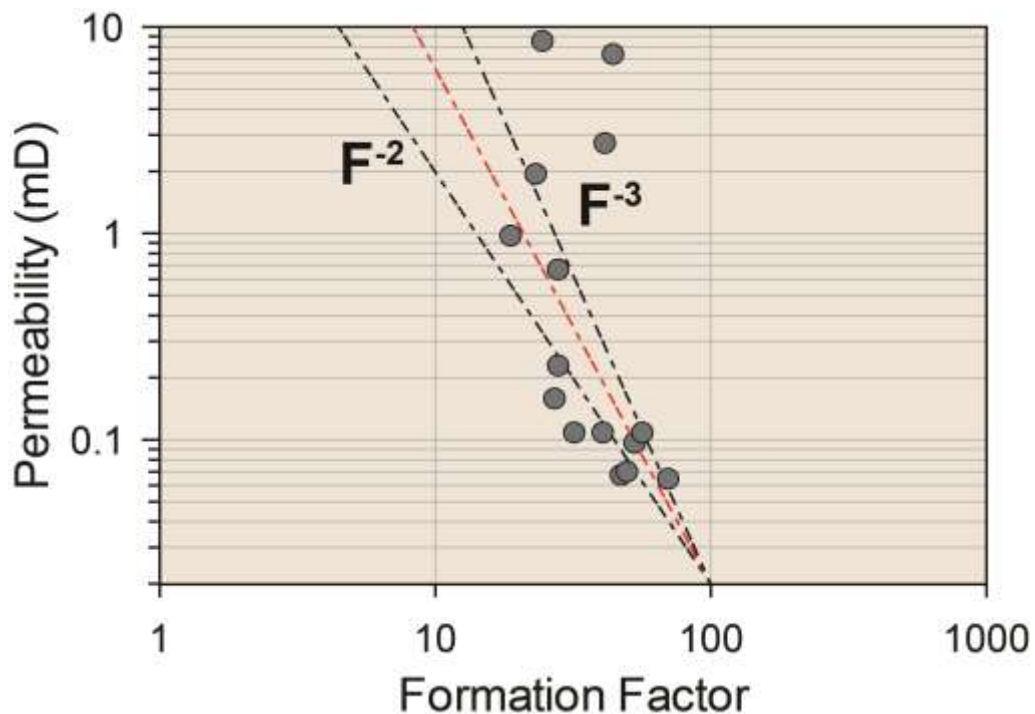
18

1 Since electrical resistivity is among the most common logging measurements, and because reservoir-
 2 scale permeability measurements are difficult to implement, the interpretation of electrical well data is
 3 able to shed light on reservoir permeability provided that both properties can be linked through the
 4 microstructural properties. The detailed characteristics of porous medium from electrical resistivity
 5 data can therefore be used to improve estimation of permeability, and to refine fluid saturation
 6 calculations in the reservoirs or aquifers. The formation factor being a resistive property, a negative
 7 correlation is expected between permeability and formation factor. A power law is frequently used to
 8 relate those two parameters (Le Ravalec et al. 1996; Casteleyn et al. 2011; Regnet et al., 2015a):

$$K \propto F^{-n}. \quad (7)$$

10

11 where n usually falls between 1 and 3. A compilation made from results published in the literature
 12 shows that linking permeability and formation factor remains a delicate process that generates large
 13 errors (figure 12). This observation also echoes to the very complex problem of equivalence between
 14 hydraulic conductivity and electrical conductivity (David, 1993).



15

16 Figure 12: Transport properties in microporous oolitic grainstones (Oolithe Blanche formation, Middle
 17 Jurassic, Paris Basin). Black dashed lines are two pilot lines drawn from the power laws with
 18 exponent -2 and -3. The red dashed line is the power law with exponent of -2.5. After
 19 Casteleyn et al. (2011), modified.

1

2 **5. Recent advances on micritic carbonate rocks**

3 A lot of work on the physical properties in carbonate rocks has been carried out on coarse-grained,
4 granular and macroporous specimens and few studies concern fine micritic carbonate series. It can be
5 explained by the low fluid recovery rates in these reservoirs, although micritic limestones exhibit large
6 variation of (1) sedimentary texture from mudstone to grainstone, (2) and facies composition. Those
7 heterogeneities imply a peculiar elastic/acoustic signature and a complex distribution of fluid flow
8 properties.

9 Those rocks are usually characterized by a microporosity fraction, which can be exclusive and reach
10 high total porosity values (50% in North Sea Chalk for example, Faÿ-Gomord et al., 2016). This
11 microporosity concerns pores smaller than 10 μm (*sensu* Lønøy (2006)) that rely on the morphology
12 and size of the micrite particles (microcrystalline calcite, Folk (1966)). The effect of such structures on
13 the physical properties of carbonates is poorly documented, except for some studies on chalk
14 formations in the North Sea (Japsen et al. 2004; Røgen et al. 2005; Fabricius et al. 2007; Gommesen et
15 al. 2007; Faÿ-Gomord et al., 2016), on micritic facies of the Urgonian formation (Lower Cretaceous)
16 of southern France (Fournier & Borgomano 2009), microporous bodies in the Middle East formations
17 (Lambert et al., 2006; Deville de Periere et al., 2011), laboratory-made micritic samples (El Husseiny
18 and Vanorio, 2016), nano-indentation tests on micritic mudstones (Saenger et al., 2016).

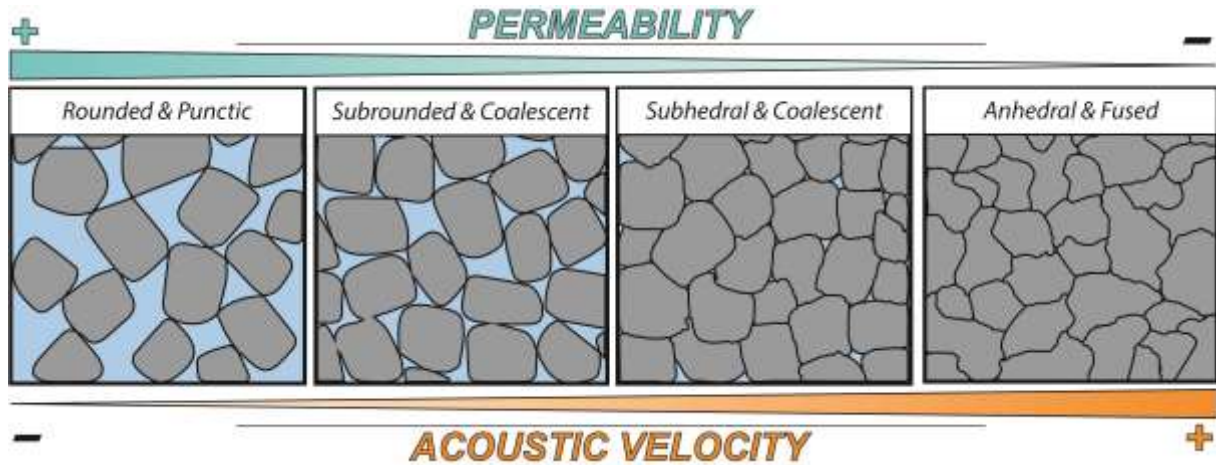
19 Here, we propose to re-explore and compare two datasets from the recent works of Casteleyn et al.
20 (2010, 2011) on the Oolithe Blanche formation and Regnet et al. (2015a, 2015b) on the Oxfordian
21 Limestones, both studies developed on the Paris Basin.

22 The Oolithe Blanche formation (middle Jurassic) which is one of the two major deep saline aquifers of
23 the Paris Basin (France) has been widely used for over forty years in geothermal energy, especially in
24 the center of the basin. Moreover, it also recently became a potential target for CO₂ geological storage
25 (Brosse et al., 2010). Past studies showed that the physical properties and the distribution of porous
26 and permeable bodies within this formation were complex (Brigaud et al., 2010; Delmas et al., 2010;
27 Vincent et al., 2011; Makhloufi et al., 2013). In addition, the heterogeneities in the distribution of
28 petrophysical properties are expressed at very different scales, from few centimeters (laboratory

1 methods) to more than one kilometer, as shown by geothermal investigations (Delmas et al., 2010).
2 The Oolithe Blanche formation is a micritic grainstone with high ooid content. Porosity is mainly
3 composed of micropores located inside those grains. Casteleyn et al. (2010, 2011) emphasised the fact
4 that the petrophysical properties of the Oolithe Blanche are mainly controlled by microstructural
5 properties, and especially by the geometry and distribution of the pore network within the grains.
6 Microporosity can be (1) uniformly distributed inside the grains resulting in fully microporous grains,
7 or (2) located on the outer part of the grains, forming a porous rim and a non-porous nucleus. For this
8 study, the samples came from outcrops located in three quarries in Burgundy, France (see Casteleyn et
9 al., 2010 for more details).

10 This Oxfordian Limestones are of primary importance since the French National Radioactive Waste
11 Management Agency (Andra) has built, within the underlying Callovo-Oxfordian clay-rich formation,
12 an underground research laboratory. They also constitute a main aquifer in the area, and constraining
13 the heterogeneity of porosity/permeability is thus a prerequisite to building a robust model from
14 seismic data for simulating fluid flows in the area. The Middle and Late Oxfordian limestones were
15 deposited in one of most important period of shallow-carbonate growth in the Paris Basin [Brigaud et
16 al., 2014]. At the beginning of the Middle Oxfordian, early coral colonization favors the development
17 of a rimmed shelf facing an open ocean. After this, during the rest of the Middle Oxfordian, an
18 isolated platform with an internal lagoonal area bounded by an ooid shoal develops. This protected
19 environment is at the origin of muddy carbonate facies. The muddy platform evolved into a ramp with
20 alternations between granular facies units, muddy facies units, and marly units (Regnet et al., 2015a).
21 Samples described in this study come from the EST205 borehole which is one of the accessing well to
22 the underground research laboratory located in the underlying clay-rich formation. They are micritic
23 microporous limestones with various textures; from mud-supported (mudstone/wackestone) to grain-
24 supported (packstone/grainstone) limestones. A major achievement of this work is the establishment
25 of the link between micrite microtexture types (particle morphology and nature of inter-crystal
26 contacts) on both acoustic and fluid flow properties. The slow increase of P-wave velocity can be seen
27 as a reflection of crystal size and growing contact cementation leading to a more cohesive and stiffer
28 micrite microtexture (figure 13). Fluid-flow properties are enhanced by the progressive augmentation

1 of intercrystalline microporosity and associated pore throat diameter (Regnet et al., 2015a), as the
 2 coalescence of micrite particle decreases between relatively coarser tight morphologies and
 3 microporous morphologies (figure 13).

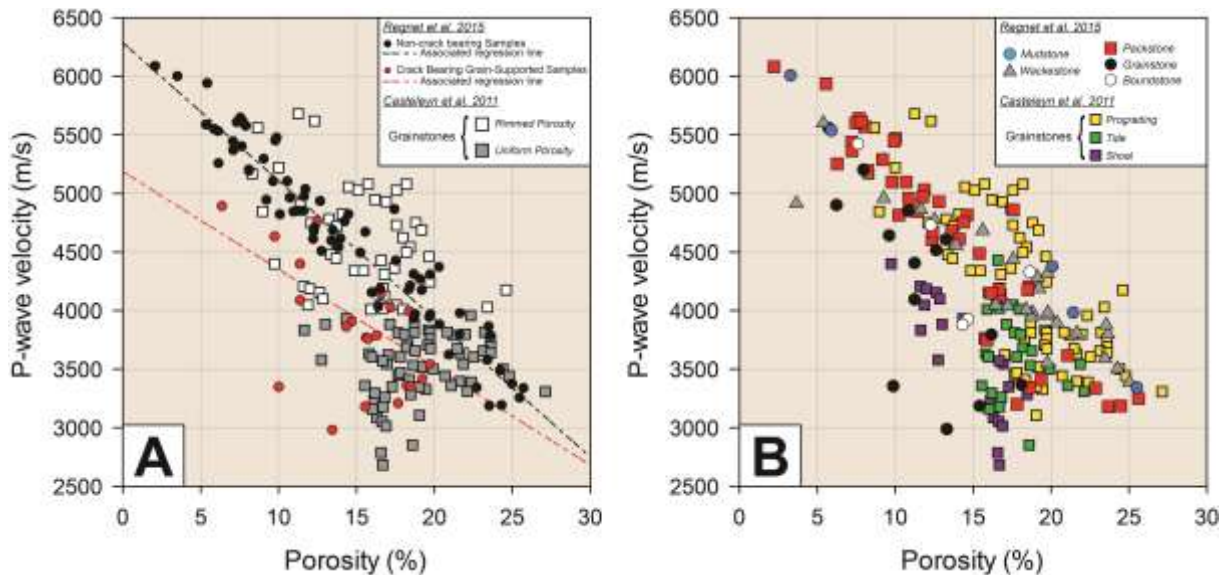


4
 5 Figure 13: Conceptual model of the Influence of micrite particle morphology and intercrystal contacts
 6 (rounded to anhedral crystals, and punctic to fused contacts, see Regnet et al., 2015a for
 7 details) on permeability and acoustic velocity (porosity in blue).
 8

9 Here, we propose to make a link between two micritic and microporous datasets using the approach on
 10 the microtextures developed by Regnet al. (2015a). Both datasets are from the eastern part of the Paris
 11 basin but from two different geological formations and settings: outcrop *versus* subsurface
 12 (boreholes).

13 This approach is not very successful for the elastic properties, probably because other controlling
 14 factors are at stake (figure 14A). The scattering observed on the P-wave velocities is explained by
 15 microcracking in the Oxfordian Limestones (Regnet et al., 2015a) and by microporosity distribution in
 16 the Oolithe Blanche (grains with rimmed porosity *versus* fully porous grains, Casteleyn et al., 2011;
 17 Regnet et al., 2015b). Such features and their effect on physical properties greatly depend on the stress
 18 state of the rocks during measurements, and the nature of the saturating fluids (Fortin et al., 2007;
 19 Guéguen et al., 2009; Regnet et al., 2015b; Borgomano et al., 2017). P and S-wave velocity increases
 20 when cracks or fractures are closed, and usually decreases during the nucleation and propagation of
 21 microcracks. Both factors (opening of microcracks and increase of crack density) would also enhance
 22 the local hydraulic conductances, resulting in an overall increase of permeability.

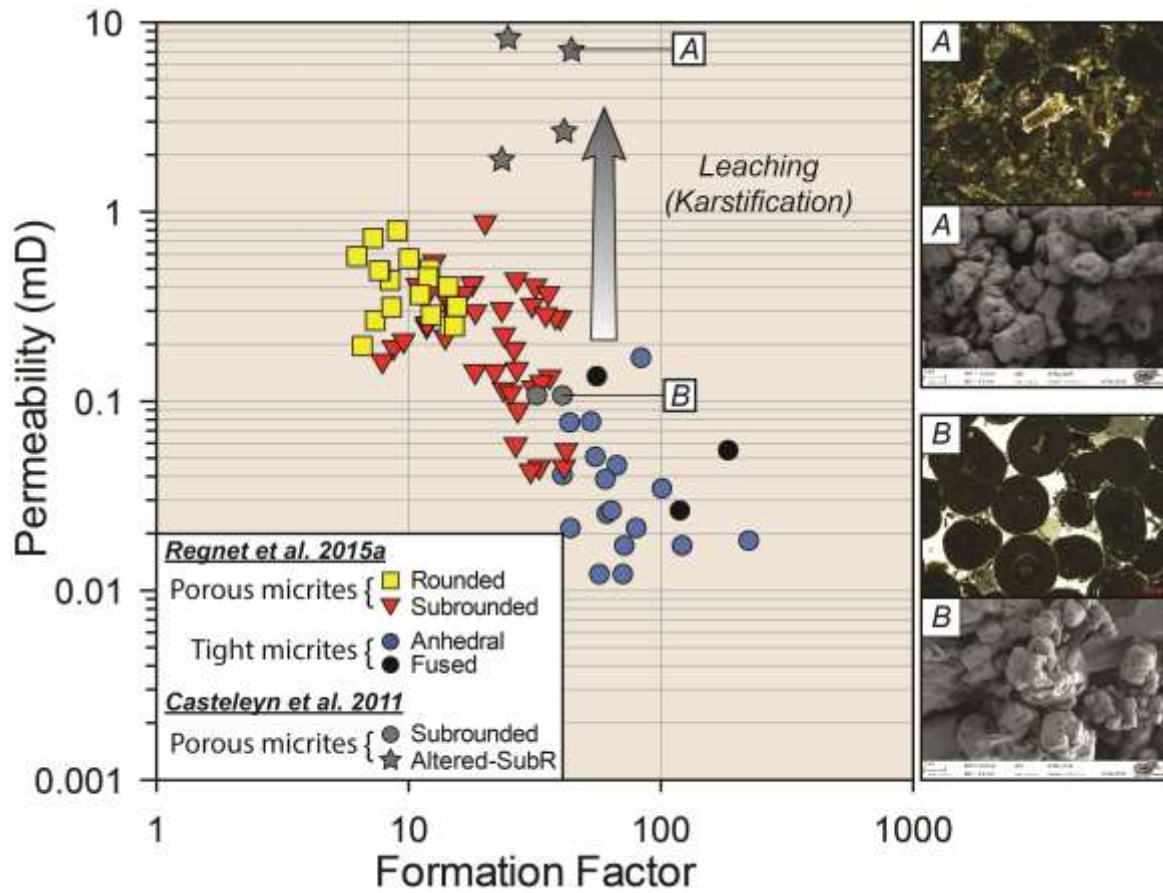
1 However, those results also show that rock-typing procedures using texture classifications such as the
 2 ones described in section 2, fail to explain the observed trends in micritic and microporous rocks
 3 (figure 14B). Micritic rock characterization has to be made at the micro-nano scale (Regnet et al.,
 4 2015a).



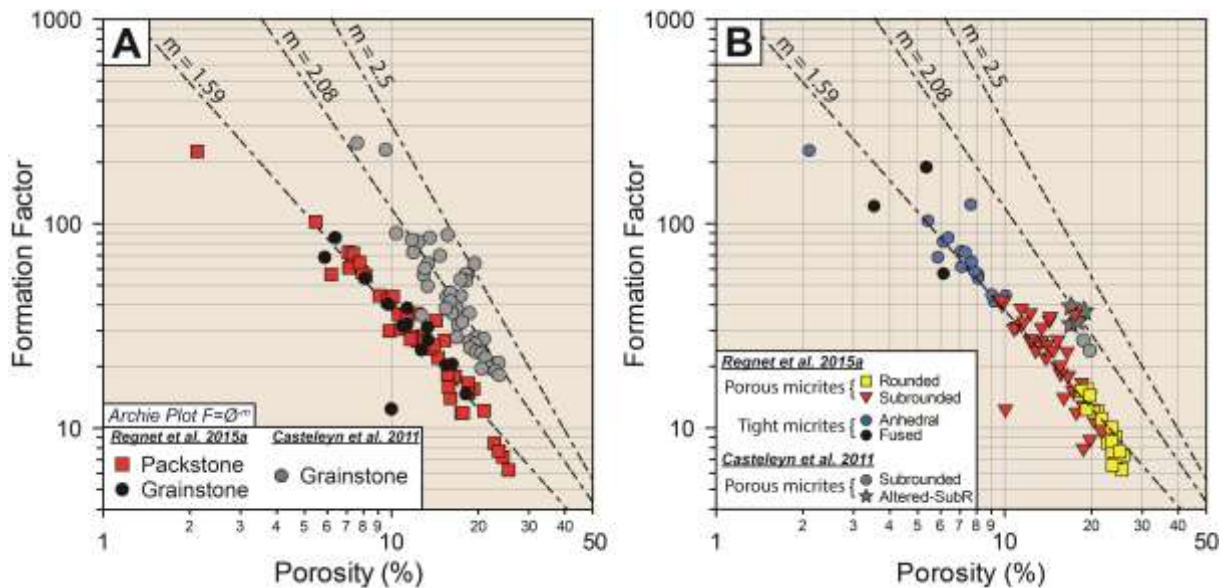
5
 6 Figure 14: P-wave velocity evolution with porosity. A – Influence of microcracks (Regnet et al.,
 7 2015a) and microporosity distribution inside the grains (Casteleyn et al., 2011). B – Influence
 8 of textures. Compilation made from Casteleyn et al. (2011) (Oolithe Blanche formation,
 9 Middle Jurassic, Paris Basin) and Regnet et al. (2015a) (Oxfordian Limestone, Paris Basin).
 10

11 When considering transport properties, the approach gives satisfying results. Microtextures observed
 12 in the Oolithe Blanche formation are characterized by similar values of permeability and electrical
 13 conductivity. The control of micrite microtextures on the transport properties is also shown by the
 14 leaching that is affecting some of the samples from Casteleyn et al. (2011) (figure 15). This late
 15 diagenesis process enhances the porous network through dissolution, as it is expected on outcrop
 16 samples, leading to higher permeability values than the subsurface samples from Regnet et al. 2015a.
 17 The log-log plot in figure 16 allows for the estimation of a mean value for the cementation exponent m
 18 taking into account grain-supported samples. By a least squares regression we find $m = 1.59$ for the
 19 data from Regnet et al. (2015) and the fit is reasonably good (black line). Samples from Casteleyn et
 20 al. (2011) are characterized by higher m value (2.08). The electrical conductivity data are not clustered
 21 by textures. This is probably due to the fact that transport properties are strongly influenced by the
 22 heterogeneity of the pore space, which can be severe even within a same sedimentological framework.

- 1 However, when displaying micrite microtextures a clear clustering appears, revealing a strong
- 2 relationship between pore space properties and micrite particle morphology.



3
 4 Figure 15: Transport properties in micritic and microporous limestones. Data points are discriminated
 5 by micrite microtextures. Subrounded morphologies from Casteleyn et al. (2011) are altered
 6 by dissolution (star-points) and are characterized by higher permeability values. Compilation
 7 made from Casteleyn et al. (2011) (Oolithe Blanche formation, Middle Jurassic, Paris Basin)
 8 and Regnet et al. (2015a) (Oxfordian Limestone, Paris Basin).
 9



1 Figure 16: Formation factor evolution with porosity in micritic and microporous limestones. Dashed
2 lines are the cementation exponent calculated from the Archie's law. A – Influence of textures.
3 B – Influence of microtextures. Compilation made from Casteleyn et al. (2011) (Oolithe
4 Blanche formation, Middle Jurassic, Paris Basin) and Regnet et al. (2015a) (Oxfordian
5 Limestone, Paris Basin).
6

7 **6. Conclusion**

8 Rock physical properties such as porosity, permeability, seismic velocity, electrical conductivity, are
9 linked through many parameters such as pore size and shape, grain contacts or cracks, pore network
10 connectivity or mineralogy. Those parameters can interact at many scales, from the microscopic scale
11 for micritic carbonate rocks, to the meter scale. Furthermore, feedback processes and coupled
12 interactions make it difficult to attribute changes in physical properties to any one parameter. The
13 early studies on those problems mostly discussed the geologic concepts surrounding carbonate pore
14 systems and presented classifications that are still widely used. Authors emphasized the importance of
15 pore space genesis, and the divisions in their classifications are genetic and not petrophysical. They
16 remain descriptive, and therefore very limited. More recent work have shown that pore space must be
17 defined and classified using geometrical factors such as size or shape in order to decipher the physical
18 information most of the time. This concerns both elastic and transport properties. Those conclusions
19 are typically true for coarse-grained, granular and macroporous specimens. When dealing with micritic
20 and microporous rocks, the micrite particle characteristics (particle morphology and nature of
21 intercrystalline contacts) are paramount to understand the physical response. This approach has been
22 successfully applied to past studies dealing with such rocks, to confirm and bring new insights into the
23 controlling parameters.

24

25 **Acknowledgments**

26 We are grateful to Lisa Casteleyn, Yasin Makhoulfi and Pierre-Yves Collin for their collaboration in
27 the project on the Oolithe Blanche formation, as well as Jérôme Fortin and Béatrice Yven; and
28 Benjamin Brigaud, for his help in the project focused on Middle Jurassic Limestones from the Paris
29 Basin. This work was supported by a research grant (Groupement National de Recherche FORMation
30 géologiques PROfondes-Programme sur l'Aval du Cycle et l'Energie Nucléaire CNRS/PACEN) given

1 to Philippe Robion and Benjamin Brigaud. We thank Phuong Nghiem for her help and advices during
2 SEM imaging at the “Plateforme Microscopie et Analyse” of the “Fédération de Recherche i-MAT
3 (FR1442)” at University of Cergy-Pontoise. We are greatly thankful to Béatrice Yven (Andra) for
4 permitting us to study the EST205 core and for providing us with material and scientific support. The
5 first author has benefitted from a PhD fellowship from the University of Cergy-Pontoise from 2011 to
6 2014. Authors are also very grateful to the two anonymous reviewers who improved the first draft of
7 the manuscript.

8

9 **References**

- 10 Archie, G. E. (1942). The electrical resistivity log as an aid in determining some reservoir characteristics.
11 Transactions of the AIME, 146(01), 54-62.
- 12 Anselmetti, F. S., Von Salis, G. A., Cunningham, K. J., & Eberli, G. P. (1997). Acoustic properties of
13 Neogene carbonates and siliciclastics from the subsurface of the Florida Keys: implications for
14 seismic reflectivity. *Marine Geology*, 144(1-3), 9-31.
- 15 Berryman, J. G. (1980). Long-wavelength propagation in composite elastic media II. Ellipsoidal inclusions.
16 The Journal of the Acoustical Society of America, 68(6), 1820-1831.
- 17 Borgomano, J. V. M., Pimienta, L., Fortin, J., & Guéguen, Y. (2017). Dispersion and attenuation
18 measurements of the elastic moduli of a dual-porosity limestone. *Journal of Geophysical Research:*
19 *Solid Earth*, 122(4), 2690-2711.
- 20 Bourbié, T., & Zinszner, B. (1985). Hydraulic and acoustic properties as a function of porosity in
21 Fontainebleau sandstone. *Journal of Geophysical Research: Solid Earth*, 90(B13), 11524-11532.
- 22 Brigaud, B., Vincent, B., Durlet, C., Deconinck, J.-F., Blanc, P., and Trouiller, A. (2010).
23 Acoustic Properties of Ancient Shallow-Marine Carbonates : Effects of Depositional Environments
24 and Diagenetic Processes (Middle Jurassic, Paris Basin, France). *Journal of Sedimentary Research*
25 80, 791-807.
- 26 Brigaud, B., Vincent, B., Carpentier, C., Robin, C., Guillocheau, F., Yven, B., and Huret, E. (2014a).
27 Growth and demise of the Jurassic carbonate platform in the intracratonic Paris Basin (France) :
28 Interplay of climate change, eustasy and tectonics. *Marine and Petroleum Geology* 53, 3-29.

- 1 Brosse, E., Badinier, G., Blanchard, F., Caspard, E., Collin, P. Y., Delmas, J., Dezayes, C., Dreux, R.,
2 Dufournet, A., Durst, P., Fillacier, S., Garcia, D., Grataloup, S., Hanot, F., Hasanov, V., Houel, P.,
3 Kervevan, C., Lansart, M., Lescanne, M., Menjoz, A., Monnet, M., P., M., Nedelec, B., Poutrel,
4 A., Rachez, X., Renoux, P., Rigollet, C., Ruffier-Meray, V., Saisset, S., Thinon, I., Thoraval, A.,
5 & Vidal Gilbert, S. (2010). Selection and characterization of geological sites able to host a pilot-
6 scale CO₂ storage in the Paris Basin (geocarbone-PICOREF). *Oil & Gas Science and Technology*.
7 65(3), 375-403.
- 8 Casteleyn, L., Robion, P., Collin, P.-Y., Menéndez, B., David, C., Desaubliaux, G., Fernandes, N., Dreux,
9 R., Badinier, G., Brosse, E., et al. (2010). Interrelations of the petrophysical, sedimentological and
10 microstructural properties of the Oolithe Blanche Formation (Bathonian, saline aquifer of the Paris
11 Basin). *Sedimentary Geology* 230, 123-138.
- 12 Casteleyn, L., Robion, P., David, C., Collin, P.-Y., Menéndez, B., Fernandes, N., Desaubliaux, G., and
13 Rigollet, C. (2011). An integrated study of the petrophysical properties of carbonate rocks from the
14 "Oolithe Blanche" formation in the Paris Basin. *Tectonophysics* 503, 18-33.
- 15 Choquette, P. and Pray, L. (1970). Geologic nomenclature and classification of porosity in sedimentary
16 carbonates. *AAPG Bulletin*, 54(2), 207-250.
- 17 Darcy H., 1858, *Les fontaines publiques de la ville de Dijon : exposition et application des principes à*
18 *suivre et des formules à employer dans les questions de distribution d'eau*. Paris, Victor Dalmont,
19 1856.
- 20 David, C. (1993). Geometry of flow paths for fluid transport in rocks. *J. Geophys. Res.* 98, 12267-12278.
- 21 Delmas, J., Brosse, E., & Houel, P. (2010). Petrophysical properties of the middle jurassic carbonates in the
22 PICOREF Sector (South Champagne, Paris Basin, France). *Oil & Gas Science and Technology*
23 *Revue de l'Institut Français du Pétrole*, 65(3), 405-434.
- 24 Deville de Periere, M., Durlet, C., Vennin, E., Lambert, L., Bourillot, R., Caline, B., and Poli, E. (2011).
25 Morphometry of micrite particles in cretaceous microporous limestones of the Middle East :
26 Influence on reservoir properties. *Mar. Pet. Geol.* 28, 1727-1750.
- 27 Digby, P.J. (1981). The Effective Elastic Moduli of Porous Granular Rocks. *J. Appl. Mech.* 48, 803-808.
- 28 Dunham, R. J. (1962). Classification of carbonate rocks according to depositional textures.

- 1 Dvorkin, J., Nur, A., and Yin, H., 1994, Effective properties of cemented granular materials: *Mechanics of*
2 *Materials*, 18, 351-366.
- 3 Eberli, G., Baechle, G., Anselmetti, F., and Incze, M. (2003). Factors controlling elastic properties in
4 carbonate sediments and rocks. *The Leading Edge* 22, 654-660.
- 5 El Husseiny, A., & Vanorio, T. (2016). Porosity-permeability relationship in dual-porosity carbonate
6 analogs. *Geophysics*, 82(1), MR65-MR74.
- 7 Fabricius, I.L., Røgen, B., and Gommesen, L. (2007). How depositional texture and diagenesis control
8 petrophysical and elastic properties of samples from five North Sea chalk fields. *Petroleum*
9 *Geoscience* 13, 81-95.
- 10 Fay-Gomord, O., Soete, J., Katika, K., Galaup, S., Caline, B., Descamps, F., ... & Vandycke, S. (2016).
11 New insight into the microtexture of chalks from NMR analysis. *Marine and Petroleum Geology*,
12 75, 252-271.
- 13 Folk, R.L. (1966). A Review of Grain-Size Parameters. *Sedimentology* 6, 73-93.
- 14 Fortin, J., Guéguen, Y., & Schubnel, A. (2007). Effects of pore collapse and grain crushing on ultrasonic
15 velocities and V_p/V_s . *Journal of Geophysical Research: Solid Earth*, 112(B8).
- 16 Fournier, F., and Borgomano, J. (2009). Critical porosity and elastic properties of microporous mixed
17 carbonate-siliciclastic rocks. *Geophysics* 74, E93-E109.
- 18 Gommesen, L., Fabricius, I. I., Mukerji, T., Mavko, G., and Pedersen, J. m. (2007). Elastic behaviour of
19 North Sea chalk : A well-log study. *Geophysical Prospecting* 55, 307-322.
- 20 Guéguen, Y., & Palciauskas, V. (1994). *Introduction to the Physics of Rocks*. Princeton University Press.
- 21 Guéguen, Y., Sarout, J., Fortin, J., & Schubnel, A. (2009). Cracks in porous rocks: Tiny defects, strong
22 effects. *The Leading Edge*, 28(1), 40-47.
- 23 Hudson, J.A., 1990, Overall elastic properties of isotropic materials with arbitrary distribution of circular
24 cracks: *Geophys. J. Int.*, 102, 465-469.
- 25 Japsen, P., Bruun, A., Fabricius, I.L., Rasmussen, R., Vejrbæk, O.V., Pedersen, J.M., Mavko, G., Mogensen,
26 C., and Høier, C. (2004). Influence of porosity and pore fluid on acoustic properties of chalk :
27 AVO response from oil, South Arne Field, North Sea. *Petroleum Geoscience* 10, 319-330.
- 28 Kenter, J., Braaksma, H., Verwer, K., and van Lanen, X. (2007). Acoustic behavior of sedimentary rocks:
29 Geologic properties versus Poisson's ratios. *The Leading Edge* 26, 436-444.

- 1 Kozeny, J. (1927). *Über kapillare leitung der wasser in boden*. Royal Academy of Science, Vienna, Proc.
2 Class I, 136, 271-306.
- 3 Kuster, G.T., and Toksöz, M.N., 1974, *Velocity and attenuation of seismic waves in two-phase media: Part*
4 *I. Theoretical formulations: Geophysics*, 39, 587-606.
- 5 Le Ravalec, M., Darot, M., Reuschle, T., & Guéguen, Y. (1996). *Transport properties and microstructural*
6 *characteristics of a thermally cracked mylonite. pure and applied geophysics*, 146(2), 207-227.
- 7 Lambert, L., Durllet, C., Loreau, J.-P., and Marnier, G. (2006). *Burial dissolution of micrite in Middle East*
8 *carbonate reservoirs (Jurassic-Cretaceous) : keys for recognition and timing. Marine and Petroleum*
9 *Geology* 23, 79-92.
- 10 Lønøy, A. (2006). *Making sense of carbonate pore systems. AAPG Bulletin* 90, 1381-1405.
- 11 Lucia, F. (1983). *Petrophysical parameters estimated from visual descriptions of carbonate rocks : a field*
12 *classification of carbonate pore space. Journal of Petroleum Technology*, 35(3), 629-637.
- 13 Lucia, F.J. (1995). *Rock-Fabric/Petrophysical Classification of Carbonate Pore Space for Reservoir*
14 *Characterization. AAPG Bulletin* 79, 1275-1300.
- 15 Lucia, F.J. (1999). *Carbonate Reservoir Characterization (Springer)*.
- 16 Lucia, F. J. (2007). *Carbonate reservoir characterization : An integrated approach. Springer*, 2nd edition.
- 17 Makhloufi, Y., Collin, P.-Y., Bergerat, F., Casteleyn, L., Claes, S., David, C., Menéndez, B., Monna, F.,
18 Robion, P., Sizun, J.-P., et al. (2013). *Impact of sedimentology and diagenesis on the petrophysical*
19 *properties of a tight oolitic carbonate reservoir. The case of the Oolithe Blanche Formation*
20 *(Bathonian, Paris Basin, France). Mar. Pet. Geol.* 48, 323-340.
- 21 Mavko, G., Mukerji, T., and Dvorkin, J. (2009). *The Rock Physics Handbook : Tools for Seismic Analysis*
22 *of Porous Media*, second edition (Cambridge University Press).
- 23 Rafavich, F., Kendall, C. S. C., & Todd, T. P. (1984). *The relationship between acoustic properties and the*
24 *petrographic character of carbonate rocks. Geophysics*, 49(10), 1622-1636.
- 25 Raymer, D. S., Hunt, E. R. et Gardner, J. S., 1980, *An improved sonic transit time-to-porosity transform:*
26 *Present at the Soc. Prof. Well Log Analysts. 21st Ann. Mtg., paper P.*
- 27 Regnet, J. B., Robion, P., David, C., Fortin, J., Brigaud, B., & Yven, B. (2015). *Acoustic and reservoir*
28 *properties of microporous carbonate rocks: Implication of micrite particle size and morphology.*
29 *Journal of Geophysical Research: Solid Earth*, 120(2), 790-811.

- 1 Regnet, J. B., David, C., Fortin, J., Robion, P., Makhloufi, Y., & Collin, P. Y. (2015). Influence of
2 microporosity distribution on the mechanical behavior of oolitic carbonate rocks. *Geomechanics
3 for Energy and the Environment*, 3, 11-23.
- 4 Regnet, J. B., Fortin, J., Nicolas, A., Pellerin, M., Guéguen, Y. (2018). Elastic properties of continental
5 carbonates: From controlling factors to an applicable model for acoustic-velocity predictions.
6 *Geophysics*, vol. 84, no. 1 (january-february 2019); P. 1–14, 15 Figs., 1 Table. 10.1190/GEO2017-
7 0344.1
- 8 Røgen, B., Fabricius, I.L., Japsen, P., Høier, C., Mavko, G., and Pedersen, J.M. (2005). Ultrasonic
9 velocities of North Sea chalk samples : influence of porosity, fluid content and texture.
10 *Geophysical Prospecting* 53, 481-496.
- 11 Saenger, E. H. (2016). Digital carbonate rock physics. *Solid Earth*, 7(4), 1185.
- 12 Verwer, K., Braaksma, H., and Kenter, J. (2008). Acoustic properties of carbonates : Effects of rock texture
13 and implications for fluid substitution. *Geophysics* 73, B51-B65.
- 14 Verwer, K., Eberli, G. P., & Weger, R. J. (2011). Effect of pore structure on electrical resistivity in
15 carbonates. *AAPG bulletin*, 95(2), 175-190.
- 16 Vincent, B., Fleury, M., Santerre, Y., and Brigaud, B. (2011). NMR relaxation of neritic carbonates : An
17 integrated petrophysical and petrographical approach. *Journal of Applied Geophysics* 74, 38-58.
- 18 Walton, K., 1987, The effective elastic moduli of a random packing of spheres: *J. Mech. Phys. Sol.*, 35,
19 213-226.
- 20 Wang, Z., & Nur, A. (1992). Elastic wave velocities in porous media: A theoretical recipe. *Seismic and
21 acoustic velocities in reservoir rocks*, 2, 1-35.
- 22 Wang, Z., 1997, Seismic properties of carbonate rocks, in I. Palaz, and K. J. Marfurt, eds., *Carbonate
23 Seismology : Society of Exploration Geophysicists Geophysical Developments* no. 6, 29-52.
- 24 Weger, R.J., Eberli, G.P., Baechle, G.T., Massafiero, J.L., and Sun, Y.-F. (2009). Quantification of pore
25 structure and its effect on sonic velocity and permeability in carbonates. *AAPG Bulletin* 93, 1297-
26 1317.
- 27 Wyllie, M.R.J., Gregory, A.R., and Gardner, L.W., 1956, Elastic wave velocities in heterogeneous and
28 porous media: *Geophysics*, 21, 41-70.
- 29 Zinszner, B., & Pellerin, F. M. (2007). *A geoscientist's guide to petrophysics*. Ed. Technip.

1
2
3
4
5
6
7
8
9
10
11
12
13
14
15
16
17
18
19
20
21
22
23
24
25
26
27

Figures Captions

Figure 1: Microstructural features and pattern in carbonate rocks at micro and nano-scale.

Figure 2: P-wave velocity evolution with porosity (saturated conditions) over a large data set (compilation by Verwer et al. (2008), modified). RHG and WTA stand for the Raymer-Hunt-Gardner's and Wyllie's Time Average trends, in red and green respectively. The Mallorca Limestone is compared with a scatter plot of 1391 samples collected from the literature.

Figure 3: P-wave velocity evolution with porosity. Data points are discriminated by the dominant pore type. The black line is the average trend for all data points (exponential best fit curve). Samples are from the ODP Site 1003 of the Great Bahama Bank. After Eberli et al. (2003), modified.

Figure 4: P-wave velocity evolution with porosity. Data points are discriminated by:

- (a) the dominant pore type from the Choquette and Pray (1970) classification
- (b) Microporosity fraction
- (c) Dominant pore size
- (d) Pore roundness
- (e) Perimeter over area of pores
- (f) Pore aspect ratios

Samples are from the Shu'aiba Formation (Middle East) and are Aptian in age, from an isolated platform of Miocene age in Southeast Asian, and from two drowned platforms on the Marion Plateau (Australia) and are also Miocene in age. After Weger et al., 2009, modified.

1
2
3
4
5
6
7
8
9
10
11
12
13
14
15
16
17
18
19
20
21
22
23
24
25
26
27
28

Figure 5: P-wave velocity evolution with porosity. Data points are discriminated by quartz fraction within the sample. Samples with high quartz fraction display lower velocities at a given porosity. Samples are from the Florida Keys formation (subsurface). After Anselmetti et al., 1997, modified.

Figure 6: P-wave velocity evolution through porosity variation. Data points are discriminated with their quartz/clay content (dot color, associated with the side colorbar) and with their dolomite content (dot size). Two mineralogical domains are individualized (calcite-dolomite mixing and calcite-quartz mixing zones). Evolution trend collected from Soete et al. (2015) showing the velocity-porosity relationship where stiff pore inclusions are dominant is also reported in the figure. After Regnet et al., 2018.

Figure 7: Influence of early cements (isopachous fringes) on the P-wave velocity evolution with porosity, Middle Jurassic Limestones from the Paris Basin. The early cementation of grainstones prevents the formation of a continuous medium, favoring wave scattering and refraction during the wave propagation. After Brigaud et al. (2010), modified.

Figure 8: Porosity-permeability evolution of carbonate rocks on a large data set. Several power-laws are represented on the graph, alongside with the porosity-permeability relationship for the Fontainebleau Sandstones. After Zinszner and Pellerin (2007), modified.

Figure 9: Porosity-permeability evolution of carbonate rocks regarding the influence of the Perimeter Over Area (PoA) of the pores, and the dominant pore size (DomSize). Samples are from the Shu'aiba Formation (Middle East) and are Aptian in age, from an isolated platform of Miocene age in Southeast Asian, and from two drowned platforms on the Marion Plateau (Australia) and are also Miocene in age. After Weger et al. (2009), modified.

1 Figure 10: Formation factor evolution with porosity. Data points are discriminated by:

2 (a) Microporosity fraction

3 (b) Perimeter over Area

4 (c) Dominant pore size

5 Black lines show the value of the cementation exponent, using equation (6). Samples are from
6 the Khuff and the Shu'aiba formations (Middle East) and are Permian and Cretaceous in age,
7 respectively; from two drowned platforms on the Marion Plateau (Australia) and are Miocene
8 in age; from the Maiella Mountain (Italy) and are Cretaceous in age. The samples from the
9 Bahamas were taken from a Holocene stromatolite. After Verwer et al. (2011), modified.

10

11 Figure 11: Dominant Pore Size and Perimeter over Area evolution in carbonate rocks. Data points are
12 characterized by the value of the cementation factor and highlight two domains of porous
13 structures and networks. Samples are from the Khuff and the Shu'aiba formations (Middle
14 East) and are Permian and Cretaceous in age, respectively; from two drowned platforms on the
15 Marion Plateau (Australia) and are Miocene in age; from the Maiella Mountain (Italy) and are
16 Cretaceous in age. The samples from the Bahamas were taken from a Holocene stromatolite.
17 After Verwer et al. (2011), modified.

18

19 Figure 12: Transport properties in microporous oolitic grainstones (Oolithe Blanche formation, Middle
20 Jurassic, Paris Basin). Black dashed lines are two pilot lines drawn from the power laws with
21 exponent -2 and -3. The red dashed line is the power law with exponent of -2.5. After
22 Casteleyn et al. (2011), modified.

23

24 Figure 13: Conceptual model of the Influence of micrite particle morphology and intercrystal contacts
25 (punctic to fused) on permeability and acoustic velocity.

26

27 Figure 14: P-wave velocity evolution with porosity. A – Influence of microcracks (Regnet et al.,
28 2015a) and microporosity distribution inside the grains (Casteleyn et al., 2011). B – Influence

1 of textures. Compilation made from Casteleyn et al. (2011) (Oolithe Blanche formation,
2 Middle Jurassic, Paris Basin) and Regnet et al. (2015a) (Oxfordian Limestone, Paris Basin).

3

4 Figure 15: Transport properties in micritic and microporous limestones. Data points are discriminated
5 by micrite microtextures. Subrounded morphologies from Casteleyn et al. (2011) are altered
6 by dissolution (star-points) and are characterized by higher permeability values. Compilation
7 made from Casteleyn et al. (2011) (Oolithe Blanche formation, Middle Jurassic, Paris Basin)
8 and Regnet et al. (2015a) (Oxfordian Limestone, Paris Basin).

9

10 Figure 16: Formation factor evolution with porosity in micritic and microporous limestones. Dashed
11 lines are the cementation exponent calculated from the Archie's law. A – Influence of textures.
12 B – Influence of microtextures. Compilation made from Casteleyn et al. (2011) (Oolithe
13 Blanche formation, Middle Jurassic, Paris Basin) and Regnet et al. (2015a) (Oxfordian
14 Limestone, Paris Basin).